

## NRC Publications Archive Archives des publications du CNRC

### **Bivalent non-human gal- $\alpha$ 1-3-gal glycan epitopes in the Fc region of a monoclonal antibody model can be recognized by anti-Gal- $\alpha$ 1-3-Gal IgE antibodies**

Hatfield, Grayson; Tepliakova, Lioudmila; Tran, Jessica; Lu, Huixin; Gilbert, Michel; Tam, Roger Y.

This publication could be one of several versions: author's original, accepted manuscript or the publisher's version. / La version de cette publication peut être l'une des suivantes : la version prépublication de l'auteur, la version acceptée du manuscrit ou la version de l'éditeur.

For the publisher's version, please access the DOI link below. / Pour consulter la version de l'éditeur, utilisez le lien DOI ci-dessous.

#### **Publisher's version / Version de l'éditeur:**

<https://doi.org/10.1080/19420862.2023.2239405>

*mAbs*, 15, 1, 2023-07-27

#### **NRC Publications Archive Record / Notice des Archives des publications du CNRC :**

<https://nrc-publications.canada.ca/eng/view/object/?id=e71305cb-eb17-4e0c-b515-eae909f4828b>

<https://publications-cnrc.canada.ca/fra/voir/objet/?id=e71305cb-eb17-4e0c-b515-eae909f4828b>

Access and use of this website and the material on it are subject to the Terms and Conditions set forth at

<https://nrc-publications.canada.ca/eng/copyright>

READ THESE TERMS AND CONDITIONS CAREFULLY BEFORE USING THIS WEBSITE.

L'accès à ce site Web et l'utilisation de son contenu sont assujettis aux conditions présentées dans le site

<https://publications-cnrc.canada.ca/fra/droits>

LISEZ CES CONDITIONS ATTENTIVEMENT AVANT D'UTILISER CE SITE WEB.

**Questions?** Contact the NRC Publications Archive team at

PublicationsArchive-ArchivesPublications@nrc-cnrc.gc.ca. If you wish to email the authors directly, please see the first page of the publication for their contact information.

**Vous avez des questions?** Nous pouvons vous aider. Pour communiquer directement avec un auteur, consultez la première page de la revue dans laquelle son article a été publié afin de trouver ses coordonnées. Si vous n'arrivez pas à les repérer, communiquez avec nous à PublicationsArchive-ArchivesPublications@nrc-cnrc.gc.ca.

REPORT



## Bivalent non-human gal- $\alpha$ 1-3-gal glycan epitopes in the Fc region of a monoclonal antibody model can be recognized by anti-Gal- $\alpha$ 1-3-Gal IgE antibodies

Grayson Hatfield<sup>a</sup>, Lioudmila Tepliakova<sup>a</sup>, Jessica Tran<sup>a</sup>, Huixin Lu<sup>a</sup>, Michel Gilbert<sup>b</sup>, and Roger Y. Tam<sup>a</sup> 

<sup>a</sup>Centre for Oncology, Radiopharmaceuticals and Research, Biologic and Radiopharmaceutical Drugs Directorate, Health Canada, Ottawa, Ontario, Canada; <sup>b</sup>Human Health Therapeutics Research Centre, National Research Council Canada, Ottawa, Ontario, Canada

### ABSTRACT

Monoclonal antibody (mAb) production using non-human cells can introduce non-human glycan epitopes including terminal galactosyl- $\alpha$ 1-3-galactose ( $\alpha$ 1-3-Gal) moieties. Cetuximab is a commercial mAb associated with causing anaphylaxis in some patients due to the binding of endogenous anti- $\alpha$ 1-3-Gal IgE to the Fab (containing bi- $\alpha$ 1-3-galactosylated glycans) but not to the Fc region (containing mono- $\alpha$ 1-3-galactosylated glycans). Despite being low in abundance in typical commercial mAbs, the inherent sensitivity of cell culture conditions on glycosylation profiles, and the development of novel glycoengineering strategies, novel antibody-based modalities, and biosimilars by various manufacturers with varying procedures, necessitates a better understanding of the structural requirements for anti- $\alpha$ 1-3-Gal IgE binding to the Fc region. Herein, we synthesized mAb glycoforms with varying degrees and regioisomers of  $\alpha$ 1-3-galactosylation and tested their binding to two commercial anti- $\alpha$ 1-3-Gal human IgE antibodies derived from a human patient with allergies to red meat (comprising  $\alpha$ 1-3-Gal epitopes), as well as to the Fc $\gamma$ R1IIIA receptor. Our results demonstrate that unexpectedly, anti- $\alpha$ 1-3-Gal human IgE antibodies can bind to Fc glycans, with bi- $\alpha$ 1-3-galactosylation being the most important factor, highlighting that their presence in the Fc region may be considered as a potential critical quality attribute, particularly when using novel platforms in mAb-based biotherapeutics.

### ARTICLE HISTORY

Received 19 May 2023  
Revised 17 July 2023  
Accepted 18 July 2023

### KEYWORDS



Glycosylation; IgE; monoclonal antibodies; non-human glycans


### Introduction

Glycosylation is an important post-translational modification of glycoproteins that can significantly affect their physical and biological properties. Monoclonal antibodies (mAbs) represent an essential class of glycoprotein-based biotherapeutics,<sup>1</sup> whose glycosylation can affect their effector activity and physicochemical stability.<sup>2</sup> mAbs comprise a dimer of heavy and light chains that form the crystallizable (Fc) and the variable (Fab) regions, in which the Fc region contains glycosylation at position N-297 of each heavy-chain monomer. A majority of commercial mAb biotherapeutic products are conventionally expressed in Chinese hamster ovary (CHO) or murine (e.g. NS0 or Sp2/0) cells, due to their ability to incorporate human-type glycans into the Fc region.<sup>3-5</sup> However, murine cells, and to lesser extent CHO cells,<sup>6,7</sup> can also incorporate non-human glycan epitopes such as the terminal galactosyl- $\alpha$ 1-3-galactosyl ( $\alpha$ 1-3-Gal) disaccharide, into their glycoproteins and glycolipids.<sup>8-11</sup> These epitopes are endogenously absent in Old World monkeys and humans, as they lack the enzymatic machinery (i.e.,  $\alpha$ 1-3-galactosyl transferase) to produce these epitopes *in vivo* and naturally have circulating anti- $\alpha$ 1-3-Gal IgG and IgM antibodies in the serum.<sup>10,12</sup> Indeed, these non-human epitopes and endogenous human antibodies present a significant obstacle in the use of pig-derived organs for xenotransplantation, as pig cells harbor a high amount of  $\alpha$ 1-3-Gal epitopes.<sup>10,13</sup> Over 10 years ago,

tick bites were discovered to induce antibody class switching to produce anti- $\alpha$ 1,3-Gal IgE antibodies, which are associated with hypersensitivity reactions including anaphylaxis.<sup>14</sup> Patients with high levels of anti- $\alpha$ 1-3-Gal IgE antibodies have been correlated to also having allergic reactions to red meats, as these animals comprise  $\alpha$ 1-3-Gal epitopes, and to the anti-cancer drug cetuximab.<sup>15</sup>

Unlike most commercially available mAbs, cetuximab, an epidermal growth factor receptor (EGFR)-targeting chimeric mouse-human IgG1 expressed in murine SP2/0 cells, is a rare exception, containing glycosylation in the Fab region. In commercially available cetuximab,<sup>16-18</sup>  $\alpha$ 1-3-Gal-bearing glycans in the Fc regions mostly contain one  $\alpha$ 1-3-Gal epitope per glycan (i.e., mono- $\alpha$ -galactosylated), while those in the Fab regions mostly comprise two  $\alpha$ 1-3-Gal epitopes on the same bi- or tri-antennary N-glycan (i.e., bi- $\alpha$ -galactosylated).<sup>16-18</sup> Previous studies reported that the presence of  $\alpha$ 1-3-Gal epitopes in the Fab region but not in the Fc region of commercially available cetuximab was responsible for binding anti- $\alpha$ 1-3-Gal IgEs.<sup>16</sup> It was hypothesized that the glycans in the Fc region were sterically inaccessible to anti- $\alpha$ 1-3-Gal IgEs, as treatment of the Fc region with Proteinase K to expose the Fc glycans regained binding capabilities.<sup>16</sup> The authors further demonstrated that bi- $\alpha$ -galactosylated glycans may be responsible for increased IgE binding in cetuximab, as exposed

**CONTACT** Roger Y. Tam  [roger.tam@hc-sc.gc.ca](mailto:roger.tam@hc-sc.gc.ca)  Centre for Oncology, Radiopharmaceuticals and Research, Biologic and Radiopharmaceutical Drugs Directorate, Health Canada, Ottawa, Ontario K1A 0K9, Canada

 Supplemental data for this article can be accessed online at <https://doi.org/10.1080/19420862.2023.2239405>

© 2023 Crown Copyright. Published with license by Taylor & Francis Group, LLC.

This is an Open Access article distributed under the terms of the Creative Commons Attribution-NonCommercial License (<http://creativecommons.org/licenses/by-nc/4.0/>), which permits unrestricted non-commercial use, distribution, and reproduction in any medium, provided the original work is properly cited. The terms on which this article has been published allow the posting of the Accepted Manuscript in a repository by the author(s) or with their consent.

mono- $\alpha$ -galactosylated Fc glycans and a linear  $\alpha$ 1-3-Gal trisaccharide (galactose- $\alpha$ 1-3-galactosyl  $\beta$ 1,4-GlcNAc) had lower binding than the bi- $\alpha$ -galactosylated Fab glycans of cetuximab.<sup>16</sup> However, the influence of the higher levels of mono- $\alpha$ -galactosylation and defined glycan structures thereof, along with the presence of bi- $\alpha$ -galactosylated glycans in the Fc region, is unclear.

Although relatively low in abundance in current commercially available mAbs,<sup>16,17</sup> the development of novel glycoengineering strategies in mAb production may affect these levels in future mAbs and alternative antibody-based modalities. For example, the biosynthesis of *N*-glycan structures during glycoprotein expression is a dynamic process and is sensitive to the relative amounts of competing glycosyltransferases<sup>19</sup> and cell differentiation;<sup>20</sup> thus, the modification of specific glycosyltransferase pathways and gene strategies may affect the activity of other glycosyltransferases, resulting in unexpected glycan structure profiles. Similarly, the *N*-glycan profile is sensitive to culture conditions during the manufacturing process, such as (but not limited to) pH, nutrient supplements, temperature, and cell type.<sup>21</sup> With the ongoing development of biosimilars by various manufacturers,<sup>22,23</sup> as well as the potential for process changes by the original innovator manufacturer to gradually change the physicochemical attributes of a product over time,<sup>24</sup> it is important to better understand the potential immunological risk associated with  $\alpha$ 1-3-galactosylation. Recent advances have resulted in more sensitive analytical techniques in glycan analysis,<sup>7,8</sup> and more defined non-human glycan structures can be distinguished from isomeric human-type glycans. For example, examination of tandem mass spectrometry (MS/MS) glycan fragmentation patterns can delineate whether isomeric biantennary glycans comprise terminal galactose residues adjacent to each other (i.e., one antenna bearing a terminal GlcNAc and the other bearing a non-human Gal- $\alpha$ 1-3-Gal- $\beta$ 1-4-GlcNAc residue) or on adjacent antennae (i.e., each antenna comprising terminal Gal- $\beta$ 1-4-GlcNAc residues as in conventional human-type glycans); similarly, it has recently been reported that terminal  $\alpha$ 1-3-Gal residues can be identified and distinguished from terminal Gal- $\beta$ 1-4-GlcNAc in denatured mAb biotherapeutics using several 2D-nuclear magnetic resonance (NMR) techniques.<sup>7</sup> However, the biological significance of specific  $\alpha$ -galactosylated *N*-glycan structures were not studied. Recent advances in glycoengineering techniques<sup>25,26</sup> have enabled a more detailed understanding of glycan structure–function relationships, with recent studies showing that the location of terminal galactose residues in biantennary complex glycans has a substantial influence on receptor binding.<sup>27,28</sup>

To this end, we herein use enzymatic glycan engineering to synthesize and incorporate various chemically defined *N*-glycan analogues with varying degrees of  $\alpha$ 1-3- and  $\beta$ 1-4-galactosylation into the Fc domain of a model mAb and report on their ability to bind to multiple anti- $\alpha$ 1-3-Gal human IgE antibodies developed from a human patient with a history of adverse reaction to red meat (which comprises  $\alpha$ 1-3-Gal epitopes) and to Fc $\gamma$ RIIIA, a receptor responsible for effector activities such as antibody-dependent cellular cytotoxicity (ADCC). Unexpectedly, we observed that unlike previous reports,<sup>15,16</sup> Fc glycans can bind anti- $\alpha$ 1-3-Gal human

IgE antibodies, although it is predominantly dictated by  $\alpha$ 1-3-Gal valency. Anti- $\alpha$ 1-3-Gal IgE antibodies are capable of binding to bi- $\alpha$ -galactosylated Fc glycans, while mono-substituted  $\alpha$ 1-3-Gal Fc glycans exhibited less binding. Our results demonstrate that the presence of multivalent  $\alpha$ 1-3-Gal epitopes in the Fc region may be a potential critical quality attribute (CQA) that warrants further attention in future novel mAb-based platforms.

## Results

### Synthesis of $\alpha$ 1-3-Galactosylated glycans

Terminal galactosylation of most human-type *N*-glycans in commercial mAbs comprise a  $\beta$ 1-4 linkage to *N*-acetylglucosamine (Gal- $\beta$ 1-4-GlcNAc) and typically exist as fucosylated mono- $\beta$ -galactosylated (i.e., G1F) and bi- $\beta$ -galactosylated (i.e., G2F) complex biantennary glycans.<sup>2,8,17</sup> However, protein expression in non-human cell types can result in further galactosylation of the  $\beta$ -galactosylated termini via an  $\alpha$ 1-3 linkage to form the non-human galactosyl- $\alpha$ 1-3-galactosyl epitope (referred herein as  $\alpha$ 1-3-Gal). To better understand the influence of  $\alpha$ 1-3-galactosylation (referred herein as  $\alpha$ -galactosylation) of Fc glycans in mAbs, we synthesized mono- and bi- $\alpha$ -galactosylated biantennary complex glycans that are found in some commercial mAb products, Figure 1.<sup>8,16</sup>

We have previously demonstrated that isolation of truncated (i.e., only one GlcNAc residue at the reducing end) biantennary glycans with regiospecific terminal mono- $\beta$ -galactosylation (1) and (2) (i.e., bearing terminal  $\beta$ -galactosylation exclusively at the  $\alpha$ 3- or  $\alpha$ 6- antenna and referred herein as G1(3)T and G1(6)T, respectively) can be achieved using conventional sialoglycoprotein (SGP) isolated from egg yolk, LacZ  $\beta$ -1,4 galactosidase, and separation by porous graphitic carbon-high performance liquid chromatography (PGC-HPLC).<sup>27</sup> With compounds (1) and (2) in hand, we prepared the  $\alpha$ 1-3-Gal analogues of the parental G1T glycans by reacting (1) and (2) with UDP-galactose and  $\alpha$ 1-3-galactosyltransferase (referred herein as  $\alpha$ 1-3-GalTase) comprising a maltose-binding domain (MBD) that was immobilized to amylose resin. Reactions were monitored by high pH anion-exchange chromatography – pulsed amperometric detection (HPAEC-PAD, Figure 2a, b) and yielded antenna-specific mono- $\alpha$ -galactosylated glycans (4) and (5), respectively. Purification by PGC-HPLC afforded the purified compounds that were confirmed by HPAEC-PAD; the relative retention times of each mono- $\alpha$ -galactosylated isomer are consistent with the parental G1T analogs, where the  $\alpha$ 6-antenna glycan eluted slightly earlier than the  $\alpha$ 3 antenna isomer,<sup>27</sup> Figure 2c. To confirm the proper installation of the  $\alpha$ 1-3-Gal epitopes, the purified products were partially reacted with  $\alpha$ 1-3,6 galactosidase, which reverted the product back to its non- $\alpha$ -galactosylated starting material (Figure 2d, e, black traces). As a negative control, mono- $\alpha$ / $\beta$ -galactosylated glycans (4) and (5) were also treated with  $\beta$ 1-4 galactosidase, which as expected, did not show any reaction since they lacked the terminal Gal- $\beta$ 1-4-GlcNAc residues (Figure 2d, e, red traces).

To prepare  $\alpha$ 1-3-Gal analogues of the parental  $\beta$ -galactosylated G2T glycan (3), reaction with  $\alpha$ 1-3-GalTase

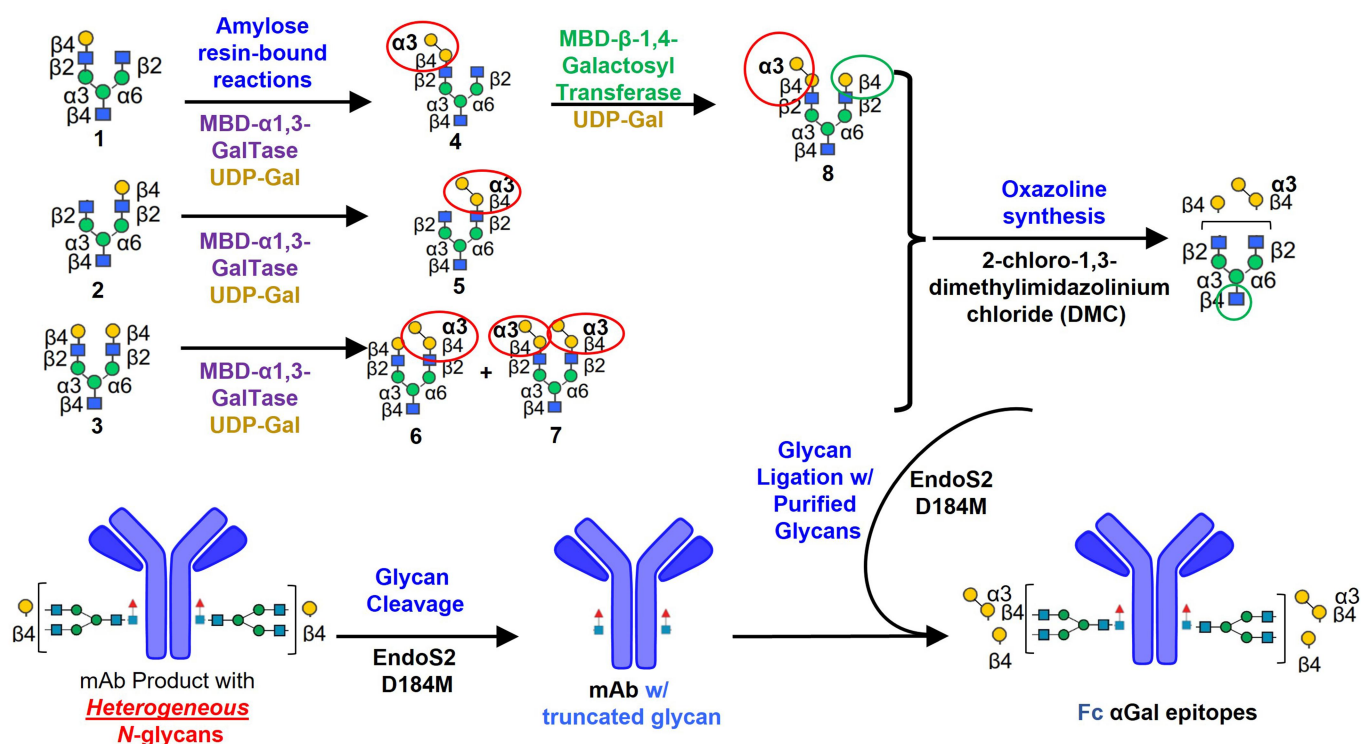


**Figure 1.** Overall synthetic scheme for a monoclonal antibody comprising various  $\alpha$ 1,3-galactosylated glycans in the Fc region. MBD- $\alpha$ 1-3-GalTase: Maltose-binding domain-conjugated  $\alpha$ 1-3-galactosyltransferase; UDP-Gal: uridine diphosphate galactose.

produced mono- and bi- $\alpha$ -galactosylated products (6–8), as detected by HPAEC-PAD and PGC-HPLC (Figure 3a–c). By PGC-HPLC, two peaks for each glycan are observed in the chromatograms, as PGC columns can separate the  $\beta$ - and  $\alpha$ -anomers of each reducing glycan;<sup>29,30</sup> following column elution, the anomers re-equilibrate to their native  $\beta$ - and  $\alpha$ -anomeric mixture in aqueous conditions. Although a single mono- $\alpha$ -galactosylated peak is observed by HPAEC-PAD (retention time at 10.5 min, Figure 3b), analysis by PGC-HPLC revealed this peak to be two different mono- $\alpha$ -galactosylated glycans ( $\beta/\alpha$  anomers at 28.5/30.8 min and 31.2/33.8 min), with a lower abundance of the earlier-eluting peaks (i.e., at 28.5/30.8 min, Figure 3c). The purified peaks were treated with either LacZ  $\beta$ 1-4-galactosidase or  $\alpha$ 1-3,6-galactosidase to map their glycan structures (Figure 3d–g).

A portion of each purified mono- $\alpha$ -galactosylated peak was partially reacted with  $\alpha$ 1-3,6-galactosidase to cleave Gal- $\alpha$ 1-3-Gal linkages and retain some of the starting material as a reference on the HPAEC-PAD chromatogram. The same parental  $\beta$ -galactosylated G2T glycan (3, Figure 3d, e, black traces) was produced following the reaction of each mono- $\alpha$ -galactosylated peak with  $\alpha$ 1-3,6-galactosidase, indicating that  $\alpha$ -galactosylation occurred on one of the two antennae in the starting materials. To identify the antenna-specificity of the  $\alpha$ 1-3-Gal epitope, mono- $\alpha$ -galactosylated glycans were treated with LacZ  $\beta$ 1-4-galactosidase to cleave the unreacted terminal Gal- $\beta$ 1-4-GlcNAc linkage (Figure 3f, g, red traces). Using the mono- $\alpha/\beta$ -galactosylated glycans (4 and 5) prepared above as a reference and a modified HPAEC-PAD method for better peak resolution, assignment of 6 and 8 is

unambiguously identified to contain the  $\alpha$ 1-3-Gal epitope on the  $\alpha$ 6 or  $\alpha$ 3-antenna, respectively. Thus, the bovine  $\alpha$ 1-3-GalTase used in this study has preferential reactivity toward the  $\alpha$ 6-antenna of biantennary glycans, similar to a previous report of another  $\alpha$ 1-3-GalTase of human origin,<sup>31</sup> but poor peak resolution (i.e., at 31 min of the PGC-HPLC chromatographs) prevented accurate relative quantification of these two isomers.

Given the poor yield of the  $\alpha$ 3 analogue (8) in the aforementioned  $\alpha$ 1-3-GalTase reaction, an alternate synthetic route was used. Glycan (4) comprising mono- $\alpha/\beta$ -galactosylation at the  $\alpha$ 3 antenna was reacted with  $\beta$ 1-4-galactosyltransferase to install the Gal- $\beta$ 1-4-GlcNAc residue at the  $\alpha$ 6 antenna (Figure 3h). Structure confirmation was achieved using LacZ  $\beta$ -1,4 galactosidase and was consistent with that shown in Figure 3g.

For the bi- $\alpha$ -galactosylated glycan (7), treatment of the purified glycan with various galactosidases confirmed the glycan structure; as expected, reaction with LacZ  $\beta$ 1-4-galactosidase showed no cleavage since the  $\beta$ -galactosyl residues were capped with  $\alpha$ 1-3-Gal epitopes (Figure 3i, red trace), while cleavage with  $\alpha$ 1-3,6-galactosidase resulted in the formation of the parental G2T (3) and mono- $\alpha$ -galactosylated glycans (6) and (8) (Figure 3i, black trace).

### Transglycosylation of $\alpha$ -galactosylated glycans into the Fc region of palivizumab

As a model mAb system to evaluate the effect of Fc- $\alpha$ -galactosylation, we used palivizumab, a prophylactic mAb targeting respiratory syncytial virus (RSV) that has the

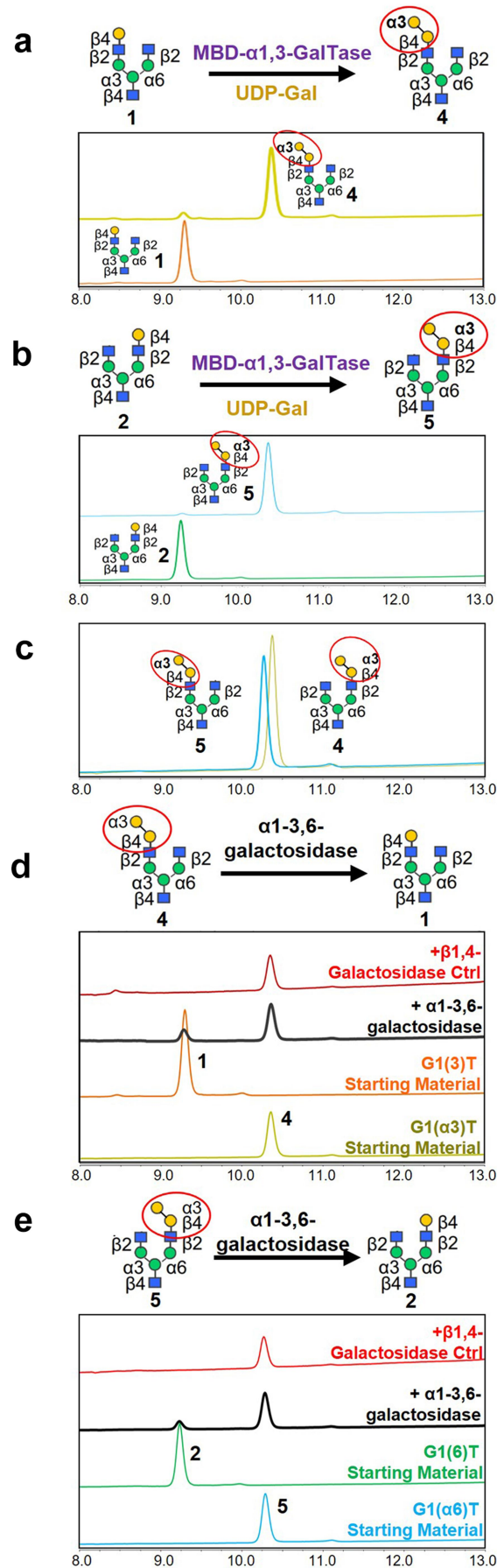


**Figure 2.** Synthesis of  $\alpha 1$ -3-Gal-containing mono- $\beta$ -galactosylated (G1T) Glycans. (a, b) Mono- $\beta$ -galactosylated glycans (**1**) and (**2**) were reacted with  $\alpha 1$ -3 galactosyltransferase (MBD- $\alpha 1$ -3-GalTase) to produce mono- $\alpha$ -galactosylated glycans (**4**) and (**5**). Overlaid HPAEC-PAD chromatograms show the starting materials and products. (c) HPAEC-PAD traces showing the purified  $\alpha 1$ -3-Gal-containing glycans (**4** and **5**) following purification by Hypercarb PGC-HPLC. (d, e) Mono- $\alpha$ -galactosylated (**4**) and (**5**) were partially degraded by  $\alpha 1$ -3,6-galactosidase (black traces) to produce compounds (**1**) and (**2**). As a negative control, starting materials were also reacted with  $\beta 1,4$ -galactosidase (red traces), which showed no reactions as expected.

same amino acid sequence of the Fc (CH2-CH3) domain as cetuximab.<sup>18,32</sup> Synthesis of fucosylated Fc glycoforms was performed using EndoS2 D184M as previously reported,<sup>27,33</sup> and reaction completion was monitored using sodium dodecyl sulfate – polyacrylamide gel electrophoresis (SDS-PAGE, Figure 4a, b). To confirm the glycan composition of the remodeled mAbs, digestion with peptide-*N*-glycosidase F (PNGase F) cleaved the glycans from the protein backbone, which were then analyzed by HPAEC-PAD (Figure 4c). Consistent with the relative retention times of truncated glycans shown in Figures 2 and 3, the fucosylated released glycans with additional galactose residues at the  $\alpha 6$  antenna eluted prior to those of the  $\alpha 3$  antenna. Interestingly, the mono- $\alpha/\beta$ -galactosylated isomers (i.e., G1( $\alpha 3$ )F and G1( $\alpha 6$ )F) eluted later than the human-type bi- $\beta$ -galactosylated glycan isomer (i.e., G2F) with the same molecular weight. As a complementary method, the released glycans were also fluorescently labeled with 8-aminopyrene-1,3,6-trisulfonate (APTS) and analyzed by capillary electrophoresis – light-induced fluorescence (CE-LIF, Figure 4d). The elution order of the  $\alpha 3$  vs  $\alpha 6$  antenna glycans was similar to HPAEC-PAD, but unlike with the HPAEC-PAD analysis, the retention time of the bi- $\beta$ -

galactosylated G2F glycan is between the two non-human mono- $\alpha/\beta$ -galactosylated glycans.

### Binding of anti- $\alpha 1$ -3-Gal IgE to Fc- $\alpha 1$ -3-Galactosylated Glycoforms

To determine the potential immunogenicity of the Fc  $\alpha 1$ -3-Gal glycan epitopes, we performed ELISA<sup>34,35</sup> using two different commercially available anti- $\alpha 1$ -3-Gal human IgE antibodies that were generated from a patient who developed allergic symptoms following intake of red meat. We used commercial cetuximab as a control, as it was reported to cause anaphylaxis in some patients with higher endogenous levels of anti- $\alpha 1$ -3-Gal IgE antibodies.<sup>15</sup> To better correlate the results of our IgE binding assay to previous reports that investigated hypersensitivity associated with commercial cetuximab,<sup>15,16,34,36</sup> we first confirmed that the relative abundance of  $\alpha$ -galactosylated glycans in our cetuximab sample is comparable to literature values of commercial cetuximab.<sup>7,16–18,37</sup> Cetuximab contains two *N*-glycosylation sites on each monomer, with one in each of the Fab and Fc regions. Glycoprofile analysis of each region was performed by first enzymatically cleaving intact cetuximab below the hinge

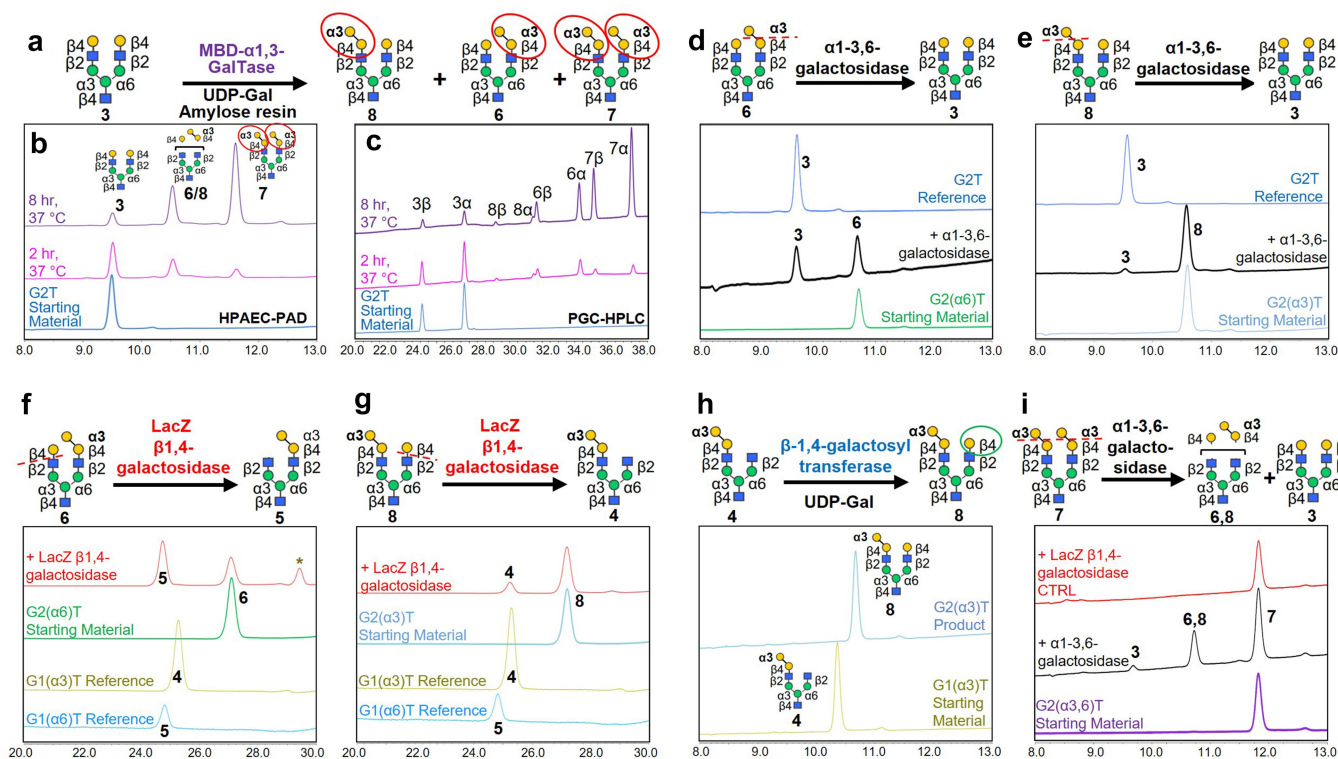


**Figure 3.** Synthesis of  $\alpha 1$ -3-Gal-containing bi- $\beta$ -galactosylated (G2T) glycans. (a) Synthetic scheme for reaction of bi- $\beta$ -galactosylated glycan (3) with  $\alpha 1$ -3-GalTase to produce mono- and bi- $\alpha$ -galactosylated glycans (6-8). Overlaid (b) HPAEC-PAD and (c) PGC-HPLC chromatographs show the starting material (blue trace), and partial reactions at 37°C after 2 and 8 h leading to the formation of  $\alpha$ -galactosylated glycans (6-8). PGC-HPLC chromatographs show the presence of  $\beta$ - and  $\alpha$ -anomers for each glycan. (d, e) Treatment of purified mono- $\alpha$ -galactosylated glycan (d) (6) and (e) (8) with  $\alpha 1$ -3,6-galactosidase (black traces) confirms the presence of an  $\alpha 1$ -3-Gal epitope. (f, g) Reaction of mono- $\alpha$ -galactosylated glycans (f) (6) and (g) (8) with LacZ  $\beta 1$ -4-galactosidase (red traces) results in the formation of compounds (5) and (4), respectively. The characteristic re-arrangement byproduct of the LacZ  $\beta 1$ -4 galactosidase reaction is denoted by an asterisk. As a reference, G1( $\alpha 3$ )T (4) and G1( $\alpha 6$ )T (5) glycans synthesized independently (i.e., from Figure 2a, b) are shown. (h) Synthesis of mono- $\alpha$ -galactosylated glycan (8) using mono- $\alpha/\beta$ -galactosylated glycan (4), UDP-Gal and  $\beta 1$ -4-galactosyltransferase. HPAEC-PAD trace of the final product is shown. (i) Bi- $\alpha$ -galactosylated (7) was partially cleaved with  $\alpha 1$ -3,6-galactosidase to produce compounds (3, 6, and 8, black trace). As a negative control, glycan (7) was also reacted with LacZ  $\beta 1$ -4-galactosidase, which showed no reactions (red trace).

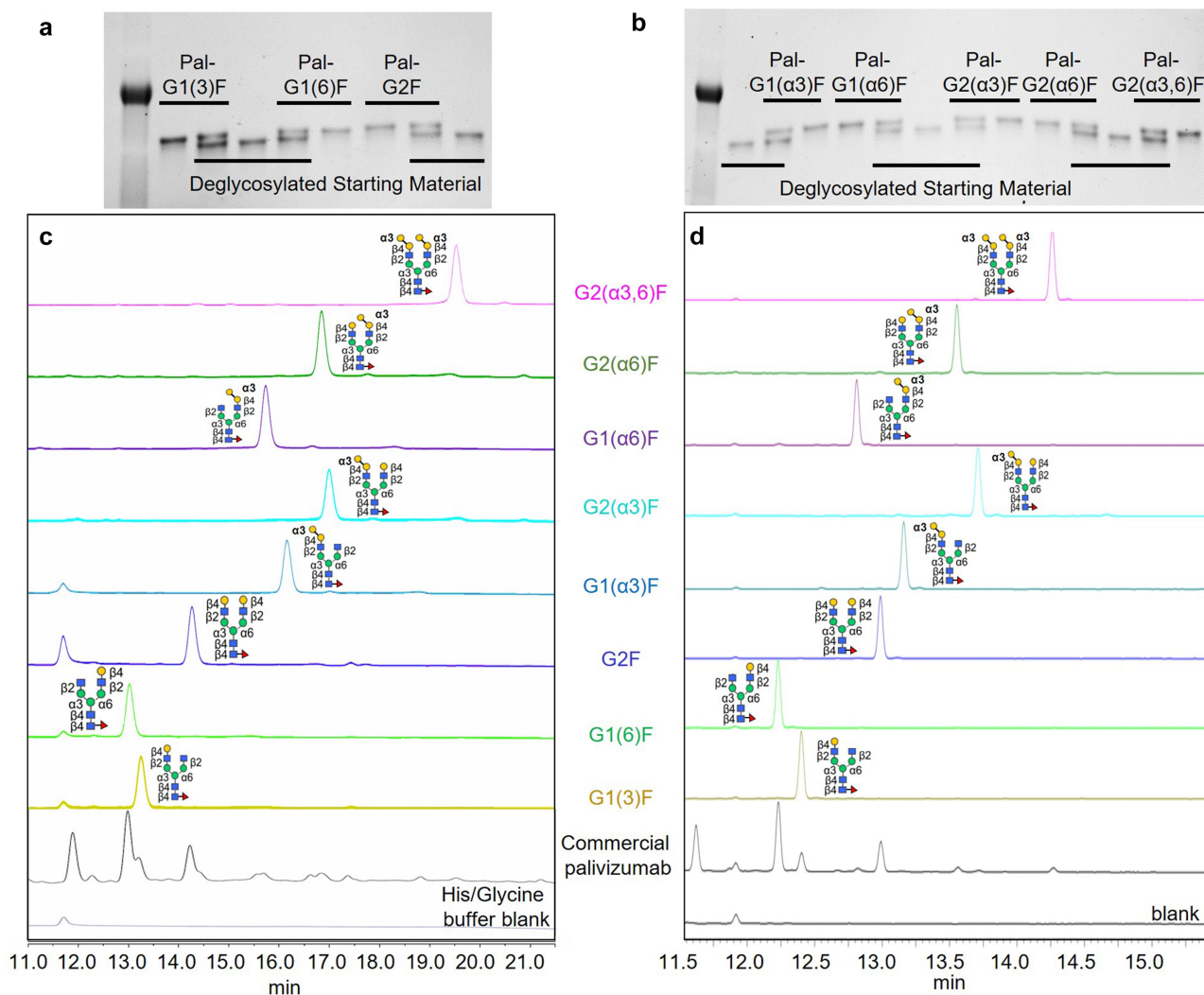


**Figure 4.** Characterization of palivizumab transglycosylated with  $\alpha$ 1–3-Gal-containing Fc *N*-glycans. (a, b) SDS-PAGE gels of palivizumab transglycosylated with (a) conventional human-type glycans and (b) non-human  $\alpha$ -galactosylated glycans, and the deglycosylated starting material (S.M.). Lanes with both product and starting materials are shown to confirm differences in band migration. A protein ladder is shown on the first lane of each gel. (c, d) Analysis of transglycosylated glycans, which were cleaved from the palivizumab protein backbone with PNGase F, and analyzed by (c) HPAEC-PAD, and (d) CE-LIF following APTS labelling. Glycans cleaved from commercial palivizumab is shown as a reference.

region with IdeZ protease, followed by Protein A affinity chromatography to separate the Fc and F(ab')<sub>2</sub> regions. Analysis by reducing SDS-PAGE shows the complete cleavage of the heavy chain into the Fab and Fc fragments (Figure S1a). Glycans were cleaved from the protein backbone using PNGase F, with the intact and F(ab')<sub>2</sub> region requiring additional cetyltrimethylammonium bromide (CTAB) as previously described (Figure S1b-d).<sup>16</sup>

HPAEC-PAD and CE-LIF were used as orthogonal methods for glycoprofile analyses of the released glycans and are consistent with the literature,<sup>7,16–18,37,38</sup> in that there is 16–20% of the biantennary bi- $\alpha$ -galactosylated glycan (i.e., G2( $\alpha$ 3,6)F) in the intact cetuximab molecule (compared to literature value of 13.3%)<sup>16</sup>, with most of it being present in the F(ab')<sub>2</sub> and not in the Fc region (less than 0.5%, Figure S2a-d, green vs red traces). Of the total F(ab')<sub>2</sub> glycans, HPAEC-PAD and CE-LIF analyses showed 27% and 34% of G2( $\alpha$ 3,6)F, respectively, and is within range of literature values of 20% to 49% using various experimental techniques;<sup>7,16–18,37,38</sup> these values are approximately

twice as much as those from intact cetuximab (Figure S2b, black traces), which corresponds to the 1:1 glycosylation ratio between F(ab')<sub>2</sub> vs Fc regions. Moreover, there is less than 4% of neutral biantennary mono- $\alpha$ -galactosylated glycans in the Fc region (Figure S2a, c, red traces) and 13% in the F(ab')<sub>2</sub> region (compared to literature values of under 7%<sup>16,18,37</sup> and 10–12%,<sup>16</sup> respectively). Less sialylated glycans were detected by CE-LIF compared to HPAEC-PAD (Figure S2e), likely due to the known loss of sialylation during the reductive amination APTS labeling process that occurs under slightly acidic conditions (i.e., our labeling protocol used 12.9% acetic acid at 60°C for 1 h).<sup>39</sup>

Next, we assessed the binding of the various  $\alpha$ -galactosylated glycoforms to two commercially available anti- $\alpha$ 1–3-Gal human IgE antibodies developed from a patient with red meat allergies by ELISA (Figure 5).<sup>34,35</sup> Following assay optimization using commercial cetuximab, all of the  $\alpha$ -galactosylated glycoforms showed greater binding than the deglycosylated or commercially available palivizumab-negative controls (gray data points), with the homogeneous

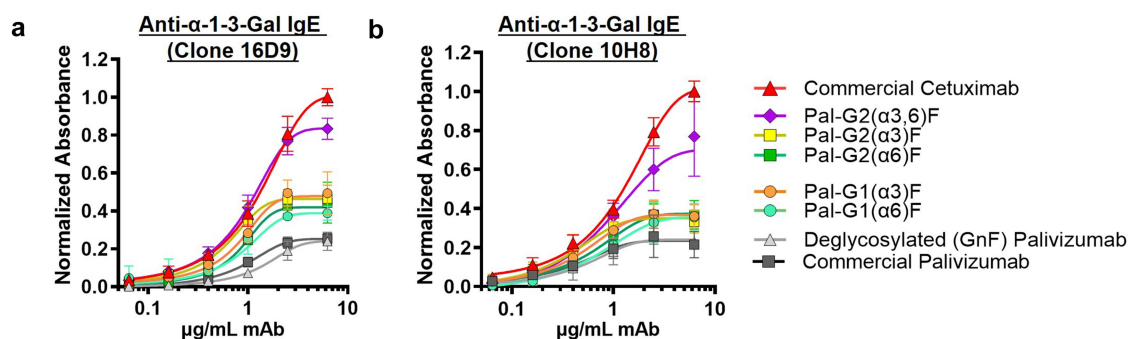


**Figure 5.** Homogeneous bi- $\alpha$ -galactosylated glycoforms in the Fc region binds to different commercially available anti- $\alpha$ 1,3-Gal IgE antibodies by ELISA. Binding to (a) clone 16D9 and (b) clone 10H8 anti- $\alpha$ 1,3-Gal IgE antibodies. Bi- $\alpha$ -galactosylated glycans (purple diamond data points) bind relatively higher than mono- $\alpha$ -galactosylated Fc glycans. Commercially available cetuximab containing 27–34% Fab bi- $\alpha$ -galactosylated glycans are shown as a comparison. Commercially available palivizumab (Synagis) and deglycosylated palivizumab are shown as negative controls (gray data points). Error bars represent mean  $\pm$  standard deviation from three separate experiments.

Fc bi- $\alpha$ -galactosylated palivizumab glycoform (i.e., Pal-G2 ( $\alpha$ 3,6)F, purple data points) having greater dose-dependent binding than the mono- $\alpha$ -galactosylated mAb glycoforms. In comparison to the commercially available cetuximab control, the bi- $\alpha$ -galactosylated Fc glycoform exhibited a greater difference in binding to the anti- $\alpha$ 1–3-Gal IgE antibody clone 10H8 compared to clone 16D9.

While we observe a slight signal increase at higher mAb concentrations (above 1  $\mu$ g/mL) in the palivizumab negative controls, a control experiment performed in the absence of any primary anti- $\alpha$ 1–3-Gal IgE antibody also showed a slight increase in signal, indicating that the secondary goat anti-IgE-horseradish peroxidase (HRP) polyclonal antibody has slight nonspecific binding to palivizumab or cetuximab IgG1 mAbs (Figure S3a); importantly, there was no difference between each sample at each concentration. As another control experiment to ensure the observed IgE binding is not due to any residual free glycans in solution, we also coated ELISA plates with 5.0  $\mu$ g/mL of deglycosylated palivizumab and added soluble G2 ( $\alpha$ 3,6)T glycans ranging from 0.35 to 22.9 nM (equivalent to 12.8 ng/mL to 3.1  $\mu$ g/mL of Fc-glycosylated mAb), followed by washing and IgE binding; we did not observe any

dose–response binding (Figure S3b), which in combination with the secondary antibody-only control experiment, confirms that the observed signals are due to anti- $\alpha$ 1–3-Gal IgE binding to mAb with immobilized G2( $\alpha$ 3,6)F glycans.

#### Binding of $\alpha$ 1–3-Galactosylated Fc glycoforms to Fc $\gamma$ RIIIA

Next, we studied the effect of homogeneous Fc  $\alpha$ -galactosylation on the binding to Fc $\gamma$ RIIIA, a receptor found in many effector cells that is predominantly responsible for antibody-dependent cellular cytotoxicity (ADCC). Consistent with previous reports of fucosylated<sup>28</sup> and defucosylated<sup>27</sup> glycans, the absence of a terminal galactose of the Gal- $\beta$ 1–4-GlcNAc residue ( $\beta$ -galactosylation) on the  $\alpha$ 6 antenna in the non- $\alpha$ -galactosylated glycoforms (i.e., Pal-G1(3)F) decreased Fc $\gamma$ RIIIA binding (Figure 6a). In comparing analogues that contained  $\alpha$ 1–3-Gal epitopes in the  $\alpha$ 3 antenna, a surprising increase in binding is observed in the mono-galactosylated  $\alpha$ 3-antenna compared to the parental Pal-G1(3)F glycoform (Figure 6b, orange circle vs. yellow triangle data), and is further increased upon addition of a terminal  $\beta$ –4 galactose residue of the  $\alpha$ 6 antenna to produce Pal-G2( $\alpha$ 3)F (Figure 6b, yellow square data points). Surprisingly, the inclusion of a second  $\alpha$ 1–

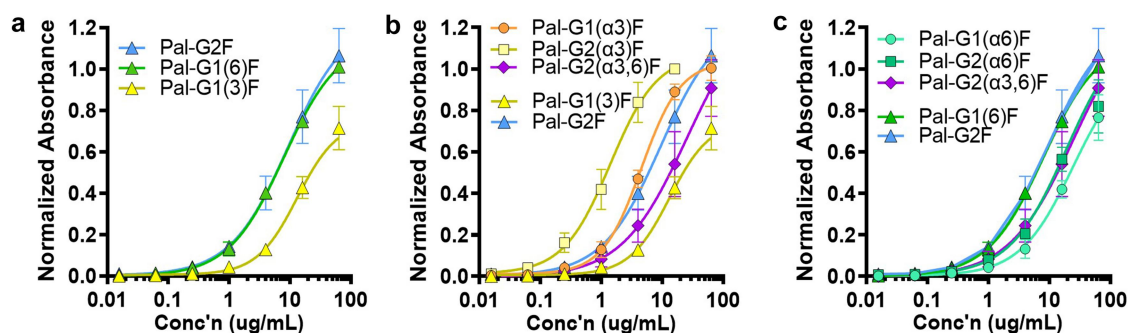


**Figure 6.**  $\alpha$ 1–3- or  $\beta$ 1–4-galactosylation on each  $\alpha$ 3 or  $\alpha$ 6 antenna differentially affects Fc $\gamma$ RIIIA binding. (a) Absence of  $\beta$ 1–4-galactosylation (Gal- $\beta$ 1–4-GlcNAc) on the  $\alpha$ 6 antenna decreases binding (G1(3)F, yellow triangle) compared to its presence (G1(6)F and G2F, green and blue triangles, respectively). (b)  $\alpha$ 1–3-galactosylation (addition of  $\alpha$ 1–3-Gal epitope) on the  $\alpha$ 3 antenna increases Fc $\gamma$ RIIIA binding (orange circles) compared to parental G1(3)F (yellow triangles), with additional  $\beta$ -galactosylation of the  $\alpha$ 6 antenna further increasing binding (yellow squares). However, addition of second  $\alpha$ 1–3-Gal epitope on the  $\alpha$ 6 antenna decreases binding (purple diamonds). (c)  $\alpha$ 1–3-galactosylation on the  $\alpha$ 6 antenna decreases binding regardless of substitution at the  $\alpha$ 3 antenna (cyan circles vs green squares vs purple diamonds) compared to parental G1(6)F and G2F (green and blue triangles, respectively). Error bars represent mean  $\pm$  standard deviation from three separate experiments.

3-Gal epitope at the  $\alpha 6$  antenna (to produce Pal-G2( $\alpha 3,6$ )F, Figure 6b, purple diamond data points) decreased its binding compared to either mono- $\alpha$ -galactosylated  $\alpha 3$ -antenna glycoforms and to the parental Pal-G2F glycoform (Figure 6b, blue triangle data points). In contrast,  $\alpha$ -galactosylation at the  $\alpha 6$  antenna (to produce Pal-G1( $\alpha 6$ )F, Pal-G2( $\alpha 6$ )F or Pal-G2( $\alpha 3,6$ )F: Figure 6c, cyan circle, green square, or purple diamond, respectively), resulted in decreased binding compared to parental Pal-G1(6)F (Figure 6c, green triangle data points). Addition of either terminal  $\alpha 1-3$  or  $\beta 1-4$  galactose residues at the  $\alpha 3$  antenna (to produce Pal-G2( $\alpha 3,6$ )F or Pal-G2( $\alpha 6$ )F, Figure 6c, purple diamond, and green square data points, respectively) only slightly increased binding compared to Pal-G1( $\alpha 6$ )F (Figure 6c, cyan circle data points), but were still less than the parental Pal-G1(6)F.

## Discussion

Detailed understanding of the relationship between glycan structure and function in biotherapeutics is crucial for evaluating which CQAs are important for the safety and potency of biotherapeutics, including mAbs. Previous insightful studies demonstrated that non-human  $\alpha 1-3$ -Gal glycan epitopes in the Fab but not in the intact Fc regions, of commercially available cetuximab could bind to hypersensitivity-associated IgE antibodies.<sup>15,16</sup> Commercial mAbs typically contain low amounts of non-human  $\alpha 1-3$ -Gal-bearing glycans, with those in the Fc region predominantly being mono- $\alpha$ -galactosylated and not bi- $\alpha$ -galactosylated.<sup>16,38</sup> Unlike most mAbs, cetuximab is a commercial mAb that also contains Fab glycans, of which some glycans in this region are bi- $\alpha$ -galactosylated.<sup>16</sup> However, the correlation between specific and chemically defined  $\alpha 1-3$ -Gal-containing glycan structures remains unclear. With the development of novel glycoengineering strategies in biopharmaceutical production,<sup>25</sup> the knowledge that altering glycosylation-related enzymes can affect other enzymes along the glycoprotein biosynthetic pathway,<sup>19</sup> and more sensitive glyco-analytical techniques that can distinguish between isomeric human vs. non-human glycans,<sup>7,8</sup> we set out to better understand specific non-human  $\alpha$ -galactosylated Fc glycans by synthesizing and characterizing various  $\alpha 1-3$ -Gal-bearing glycans that are found in the Fc region of commercial mAbs.

Using chemoenzymatic transglycosylation and enzymatic glycan semi-synthesis, we synthesized  $\alpha$ -galactosylated analogues of fucosylated Fc glycans typically found in commercial mAbs.<sup>5,16,17,38</sup> For example, commercial palivizumab and infliximab had been reported to include mono- and bi- $\alpha$ -galactosylated G1F and G2F in amounts ranging from 1.1% to 5.1%.<sup>16</sup> Following the enzymatic transglycosylation of a model mAb palivizumab (bearing the same Fc domain sequence as cetuximab) with EndoS2 D184M to produce homogeneous  $\alpha 1-3$ -Gal-containing mAbs, the various glycoforms were assessed for their ability to bind to anti- $\alpha 1-3$ -Gal human IgE antibodies. These were developed from IgE-producing B cells from a human patient, with red meat allergies using hybridoma technology to produce allergen-specific IgE with natural pairing of the heavy and light chains that forms the IgE response in allergic patients.<sup>40,41</sup> The biological relevance of IgE antibodies produced using this technique has

been demonstrated with the human IgE mAb (2F10) derived from an allergic patient to dust mite allergen (Der p2),<sup>42</sup> which inhibited the binding of the Der p2 antigen to polyclonal IgE from allergic patients' sera, indicating that IgE mAb 2F10 is an important part of the human IgE polyclonal response to Der p2; in comparison, mutant IgE mAbs with mutations in the binding epitopes showed reduced binding inhibition. In other experiments, a human Fc $\epsilon$ RI $\alpha$ -transgenic mouse model of passive systemic anaphylaxis was used to demonstrate that these<sup>42</sup> and other similar IgE mAbs<sup>43</sup> were able to contribute to systemic anaphylaxis. As our aim was to compare the relative IgE binding of Fc- $\alpha$ -galactosylated glycans with commercial cetuximab to which there is clinical evidence to cause anaphylaxis via IgE binding, we performed ELISA to detect IgE binding, a method that has been previously reported to correlate high anti-cetuximab IgE levels from the serum of cetuximab-treated patients with the risk of severe hypersensitivity reactions and anaphylaxis.<sup>34,35</sup>

Our results demonstrate that the presence of homogeneous monovalent  $\alpha 1-3$ -Gal non-human epitopes in the Fc region possesses low binding to  $\alpha 1-3$ -Gal human IgE antibodies and is only slightly higher than the negative controls, deglycosylated or commercially available palivizumab, of which anaphylaxis of the latter is reportedly rare.<sup>44,45</sup> The location of the  $\alpha 1-3$ -Gal epitope or the addition of Gal- $\beta 1-4$ -GlcNAc on either antenna of the biantennary Fc glycans does not influence anti- $\alpha 1-3$ -Gal human IgE binding. These data are consistent with previous reports that mono- $\alpha$ -Fc glycosylation in commercial mAbs (comprising less than 10% of total glycans) do not bind anti- $\alpha 1-3$ -Gal IgE,<sup>16</sup> and we now further show that increasing the degree of substitution of any of the mono- $\alpha$ -galactosylated glycans prepared in this study does not increase its binding to levels comparable to commercial cetuximab. Surprisingly, introduction of a second  $\alpha 1,3$ -Gal epitope to the same glycan to produce the bi- $\alpha$ -galactosylated Fc-glycoform showed greater dose-dependent binding to two different commercially available anti- $\alpha 1-3$ -Gal human IgE antibodies (clones 16D9 and 10H8), although at slightly lower levels than an equimolar amount of cetuximab protein (which contains 27–34% of the same bi- $\alpha$ -galactosylated glycan in the Fab region).

While there was a greater difference with the bi- $\alpha$ -galactosylated Fc-glycoform compared to commercial cetuximab in binding to the 10H8 IgE antibody, our data nonetheless show that bi- $\alpha$ -galactosylation at the Fc region can indeed be recognized by multiple anti- $\alpha 1-3$ -Gal human IgE antibodies, which is in contrast to previous reports that  $\alpha 1-3$ -Gal-bearing glycans of intact Fc regions cannot be recognized by IgE antibodies.<sup>16</sup> Palivizumab and cetuximab have the same sequence of their Fc domains, and our previous report<sup>27</sup> showed that the enzymatic transglycosylation process is able to maintain the glycan–protein interaction of the  $\alpha 6$ - and not the  $\alpha 3$ -antenna of the biantennary glycans, consistent with other NMR and X-ray diffraction studies of native Fc domains;<sup>46–48</sup> thus, the binding of anti- $\alpha 1-3$ -Gal human IgE to Fc  $\alpha$ -Gal glycans in our palivizumab model is appropriate to be compared to previous studies using native cetuximab.<sup>16</sup> While previous data such as X-ray diffraction<sup>46</sup> provided evidence that the glycan was generally 'shielded' within the CH2 Fc domain, X-ray diffraction captures a stabilized conformation, which

may not directly reflect a glycoprotein's dynamic nature in solution. NMR studies provide a technique to analyze the dynamic nature of a protein in solution, and several studies<sup>47,48</sup> showed that portions of the glycans are dynamic and are exposed to the external solvent; in particular, the "α3" antenna of a biantennary glycan is exposed, while the α6 antenna interacts more with the polypeptide backbone. Detailed work by Barb and Prestegard<sup>47</sup> further showed that α6-antenna interaction with the peptide backbone is not static and has temperature-dependent mobility. These latter data provide more rationale as to how the non-reducing termini of glycans within the Fc domain can be recognized and processed by glycan-modifying enzymes.<sup>49</sup> These data also support our findings that Fc glycans comprising α1-3-Gal epitopes can be recognized by anti-α1-3-Gal human IgE antibodies, although the poor binding of mono-α-galactosylated glycans demonstrates that increasing valency of α1-3-Gal epitopes in Fc glycans is the dominant factor that influences IgE binding.

The ability to set a threshold for the number of α-Gal epitopes found in a therapeutic drug is of important interest to manufacturers to ensure biotherapeutic products do not produce adverse side effects. However, setting such a threshold is complicated by the limited data on these rare but dangerous adverse effects. While studies have been performed to correlate anti-α1-3-Gal IgE levels with hypersensitivity reactions in cetuximab-treated patients,<sup>34,35,50</sup> the heterogeneous nature of α-Gal glycans in commercial cetuximab limits the use of these data to set definitive α-Gal thresholds. Our data suggest that specific glycan structures (as opposed to overall α-galactosylation levels) should be considered and may be a more suitable criterion for setting a threshold for α-Gal epitopes during product development. Further work to determine the no/lowest observed adverse effect levels (NOAEL or LOAEL) of α-Gal epitopes in cetuximab-treated patients (especially those from escalating low-dose studies) could serve as a benchmark or reference dose to set as a threshold for potential hypersensitivity from cetuximab. To define the threshold of specific α-Gal glycans that are acceptable in a product, chemically defined and homogenous α-Gal glycans could then be compared to the benchmark dose to evaluate the relative activity of each α-Gal glycan using multiple orthogonal bioassays (e.g., *in vitro* cell studies and *in vivo* humanized FcεRIa mouse models of anaphylaxis).

To further understand the properties of Fc-α-galactosylation on binding to a key receptor involved in effector activity, we assessed binding to FcγRIIIA. Our data showed contrasting effects of mono-α-galactosylation of Pal-G1F and Pal-G2F on binding, where the addition of a single α1-3-Gal epitope at the α3 antenna (i.e., Pal-G1(α3)F and Pal-G2(α3)F) increased binding, while addition to the α6 antenna resulted in lower binding compared to the parental Pal-G2F glycoform. Incorporation of α1-3-Gal epitopes to both antennae to produce the bi-α-galactosylated glycan (i.e., Pal-G2(α3,6)F) abrogates the increased FcγRIIIA binding seen in the Pal-G2(α3)F analogue. Previous work with fucosylated Fc glycans showed that the Gal-β1-4-GlcNAc residue of the α3 antenna is more exposed to the solvent and has high glycan mobility, whereas these residues of the α6 antenna interact with the Fc protein backbone to decrease glycan mobility;<sup>47</sup> the relationship between glycan mobility and

receptor binding was subsequently directly correlated.<sup>51</sup> Thus, it is possible that the addition of an α1-3-Gal epitope to Gal-β1-4-GlcNAc of the α6 antenna causes destabilizing interactions with the Fc protein backbone to increase the glycan mobility. Based on the X-ray structure of the Gal-β1-4-GlcNAc residue of the α6 antenna in Fc glycans (PDBID: 4byh), the C3 position of the galactose residue is in close proximity to the protein backbone, thus incorporating an α1-3-Gal residue at this position is likely to perturb glycan backbone interactions and increase glycan mobility.<sup>52</sup> However, how the inclusion of an α1-3-Gal epitope to the conventionally solvent-exposed and more mobile α3 antenna increases binding to FcγRIIIA is more puzzling. It could either form new protein backbone interactions to decrease glycan mobility or directly interact with the FcγRIIIA receptor itself. As β-galactosylation of the α6 antenna interacts with the protein backbone to decrease the glycan motion, the increased activity of the G2(α3)F analogue compared to G1(α3)F (that lacks β-galactosylation at the α6 antenna) suggests that glycan mobility remains an important component of this increased binding mechanism. Exact mechanisms will require more detailed examination and are beyond the scope of this work. As a comparison, the change in binding to FcγRIIIA upon addition of α1-3-Gal epitopes to terminal Gal-β1-4-GlcNAc residues is different from the results observed with the addition of *N*-acetyl-neuraminic acid to terminal Gal-β1-4-GlcNAc residues. Analogous bi-β-galactosylated glycans (i.e., G2F) with terminal mono-<sup>49,53</sup> and di-sialylation<sup>54</sup> showed comparable binding to FcγRIIIA compared to their desialylated G2F analogue,<sup>53,54</sup> although the di-sialylated glycoform showed a moderate decrease in ADCC activity *in vitro*.<sup>33</sup>

In conclusion, our results demonstrate the unique binding activities of two Fc-α-galactosylated analogues. Mono-α-galactosylation of the α3 antenna increases FcγRIIIA binding compared to its parental non-α-galactosylated glycans, with additional β-galactosylation at the α6 antenna further increasing activity. However, the set of mono-α-galactosylated glycans displayed only a slight increase in binding to anti-α1-3-Gal human IgE antibodies compared to commercial or deglycosylated palivizumab controls. In contrast, the bi-α-galactosylated Fc glycoform has decreased receptor binding to FcγRIIIA receptors compared to its parental non-α-galactosylated glycoform, potentially due to disruption of glycan-protein backbone interactions of the former; moreover, they can indeed be recognized by anti-α1-3-Gal IgE antibodies, and while bi-α-1,3-galactosylated glycans are in low abundance in current commercially available mAb products, our data demonstrate that their presence in the Fc region cannot be overlooked in establishing CQAs for novel platforms and biosimilars in mAb-based biotherapeutics.

## Materials and methods

### Enzyme expression

*α1-3-Galactosyltransferase*. Construct BOV-13 contains the sequence encoding aa 81–368 of the bovine α1-3-galactosyltransferase (referred herein as α1-3-GalTase, GenBank #NP\_803477 with mutation D197N) cloned in plasmid pCWori+ that also encodes the maltose-binding protein

(upstream of the  $\alpha$ -1,3-galactosyltransferase). *Escherichia coli* AD202 (Coli Genetic Stock Center (CGSC), Cat# 7297) containing the construct BOV-13 was grown in 2 $\times$  YT medium (Fisher, Cat# BP2467–500) containing 150  $\mu$ g/mL ampicillin (Fisher, Cat# BP1760–25) and 2 g/L glucose (Sigma, Cat# 7021-1 KG). The culture was incubated at 37°C until A600 = 0.35, induced with 0.5 mM isopropyl 1-thio- $\beta$ -D-galactopyranoside (IPTG, Fisher, Cat# BP1755–1), and then incubated overnight at 25°C, 200 rpm. The cells were broken by repeated freeze/thaw cycles using dry ice and ethanol: cells in flasks were placed in a dry ice/ethanol bath for 2 min, followed by 8 min in a water/ice bath, and repeated three times; cells in flasks were let to stand on ice for another 30 min, followed by centrifugation at 4000  $\times$  g for 15 min. Supernatant containing the BOV-13  $\alpha$ 1–3-GalTase was purified by affinity chromatography on amylose resin following the manufacturer's instructions (New England Biolabs, Cat # E8021S) with the following modification: following incubation and immobilization with amylose resin, the resin with bound  $\alpha$ 1–3-GalTase was rinsed several times with  $\alpha$ -Gal buffer (100 mM Tris buffer, 100  $\mu$ M MnCl<sub>2</sub>, pH 7.0) and stored in this solution at the same resin concentration as initially supplied, at 4°C until use.

**$\beta$ 1–4-galactosyltransferase.** Construct HP-21 is a recombinant version of the HP0826  $\beta$ -1,4-galactosyltransferase from *Helicobacter pylori* cloned in plasmid pCWori+. The  $\beta$ -1,4-galactosyltransferase was produced in *E. coli* AD202 containing the construct HP-21 and grown in 2 $\times$  YT medium using IPTG as the inducer. The cells were resuspended in 50 mM HEPES pH 7.5 and 0.5 M NDSB-201 (Calbiochem, Cat# 480005–25 GM). The cells were broken using an Avestin C5 Emulsiflex cell disruptor (Avestin, Ottawa) and the extract was centrifuged at 27,000  $\times$  g for 30 min at 4°C. The supernatant was then centrifuged at 208,000  $\times$  g for 1 h at 4°C.  $\beta$ -1,4-galactosyltransferase was partially purified by precipitation with (NH<sub>4</sub>)<sub>2</sub>SO<sub>4</sub> at a final concentration of 1.65 M and incubation on ice for 100 min. The precipitate was recovered by centrifugation at 17,000  $\times$  g for 20 min at 4°C. The pellet was resuspended in 50 mM HEPES, pH 7.5, 0.1 M NaCl and dialyzed extensively against the same buffer.

**EndoS2 D184M endoglycosidase.** Sequence aa 1–843 of EndoS2 from *S. pyogenes*<sup>55</sup> (containing the D184M mutation)<sup>33</sup> and a C-terminal decahistidine tag was cloned into a pET-20b(+) vector and transformed into BL21 (DE3) pLysS *E. coli* (Fisher, Cat# PRL1195). *E. coli* containing the EndoS2 D184M vector was then grown in LB media (Fisher, Cat# BP1427–500) with ampicillin at 37°C. EndoS2 D184M was produced following induction with IPTG and cultured overnight with shaking at 16°C. Cells were then centrifuged at 4000  $\times$  g (4°C, 45 min), and the resulting pellet was resuspended in Binding Buffer (100 mM sodium phosphate, 10 mM Tris base buffer, pH 8.0) with 20 mM imidazole (Sigma, Cat# I202-100 G). Cells were lysed using freeze/thaw method as described above, and the supernatant was purified using Ni-NTA affinity chromatography. Following binding of the protein to the Ni-NTA resin (Sigma, Cat# 70691–4), the resin was washed with six column volumes of Binding Buffer with 20 mM imidazole, and then Binding Buffer with 60 mM imidazole. EndoS2 D184M was eluted

using an elution buffer comprising 100 mM sodium phosphate, 10 mM Tris base buffer with 240 mM imidazole (pH 8.0) for four column volumes into separate fractions. SDS-PAGE (BioRad, 10% Mini-PROTEAN® TGX Stain Free™ Protein Gels, Cat# 4568034 or 4,568,036) was used to confirm protein elution, and purified fractions were combined and buffer exchanged into phosphate-buffered saline (PBS) pH 6.0.

### Synthesis of $\alpha$ 1–3-Galactosylated glycans

$\beta$ -galactosylated glycan starting materials (1)–(3) were prepared as previously described.<sup>27</sup> In brief, SGP was isolated from egg yolk purchased from a local grocery store, and washed several times by vigorous stirring with diethyl ether. After removal of diethyl ether washes, the remaining precipitate was extracted with 40% acetone, filtered, and further extracted and washed with 40% acetone. Following evaporation of acetone, the remaining solution was passed through an activated carbon column plug, and sequentially washed with Milli-Q (MQ) water containing 0.1% trifluoroacetic acid (TFA) and 5% acetonitrile (with 0.1% TFA). Sialylated glycans were eluted with 25% acetonitrile (with 0.1% TFA), evaporated, and lyophilized. Truncated mono- (1, G1(3)T) and bi- $\beta$ -galactosylated (3, G2T) glycans were obtained following the treatment of SGP with  $\alpha$ 2–3,6,8,9-neuraminidase (New England Biolabs, Cat# P0720S) to cleave sialic acids and EndoS containing a chitin-binding domain (New England Biolabs, Cat# P0741) immobilized to chitin resin (New England Biolabs, Cat# S6651) to release glycans from the peptide backbone.<sup>27</sup> Purification was performed using PGC-HPLC as described below. To obtain the mono- $\beta$ -galactosylated glycan at the  $\alpha$ 6 antenna (2, G1(6)T), G2T glycan (3) was treated with LacZ  $\beta$ 1–4-galactosidase (Sigma, Cat # 10105031001) as previously described and similarly purified by PGC-HPLC.<sup>27</sup>

To synthesize the  $\alpha$ 1–3 galactosylated glycans (4–7), 2.0  $\mu$ mol  $\beta$ -galactosylated glycans were diluted in 100  $\mu$ L of  $\alpha$ -Gal buffer and 4.0  $\mu$ mol of UDP-galactose (Sigma, Cat# 670111) was added and adequately mixed. 50  $\mu$ L of slurry containing  $\alpha$ 1–3-GalT-amylose-resin was then added, and the reaction was incubated overnight at 37°C. Completion of reactions was monitored using HPAEC-PAD, as described below. To prepare mono- $\alpha$ - and bi- $\beta$ -galactosylated glycan (8, G2( $\alpha$ 3)T), 1.4 mg (1.0  $\mu$ mol) of the mono- $\alpha$ / $\beta$ -galactosylated glycan (4) was diluted in 440  $\mu$ L of  $\alpha$ -Gal buffer, 2.0 mg (3.23  $\mu$ mol) of UDP-Gal was added and mixed, followed by addition of 88  $\mu$ L of  $\beta$ 1–4-galactosyltransferase stock solution. Purifications of all  $\alpha$ -galactosylated glycans were performed by HPLC using a Hyper Carb column as described below.

To characterize the linkage of galactose residues, enzymatic reactions with LacZ  $\beta$ 1–4 galactosidase or  $\alpha$ 1–3,6 galactosidase (New England Biolabs, Cat# P0731) were used. For LacZ  $\beta$ 1–4 galactosidase, 8  $\mu$ L of glycan solution was mixed with 1  $\mu$ L of enzyme, 1  $\mu$ L of 500 mM KCl, and 1  $\mu$ L GlycoBuffer 1 (New England Biolabs, Cat# B1272S) and incubated overnight at

37°C. For  $\alpha$ 1-3,6-galactosidase reactions, 8  $\mu$ L of glycan solution was mixed with 1.0  $\mu$ L of enzyme and 1.0  $\mu$ L GlycoBuffer 1, and incubated overnight at 37°C.

Glycans were converted into their respective oxazoline derivatives as previously described.<sup>27</sup> Briefly, they were reacted with 2-chloro-1,3-dimethylimidazolium chloride (DMC, Sigma, Cat# 529249-25 G) and triethylamine (TEA, Fisher, Cat# 0484-100) for 45 min at 4°C and then immediately purified by passing through a Sephadex G25 column (Fisher, Cat # 45-002-048) pre-equilibrated with 0.01%  $\text{NH}_4\text{OH}$ . A portion of each collected fraction was diluted into 10 mM NaOH and monitored for purity by HPAEC-PAD. Pure fractions were combined, quantified, aliquoted, and lyophilized for storage at  $-80^\circ\text{C}$ .

### **Monoclonal antibody transglycosylation**

Transglycosylation procedures for palivizumab (Synagis®, AbbVie, DIN#02438364, purchased from McKesson Pharmacy) were adapted from previously reported work,<sup>27</sup> with the following modifications. Briefly, for 0.5 mg (3.43 nmol) palivizumab, deglycosylation was first performed at 10 mg/mL using 5.0  $\mu$ g EndoS2 D184M,<sup>33</sup> in a final volume of 50  $\mu$ L of transglycosylation buffer (TGB, 50 mM Tris, pH 7.3). The reaction was incubated overnight at 37°C, and completion was monitored by SDS-PAGE. To perform the transglycosylation reactions, the solution comprising EndoS2 D184M and deglycosylated palivizumab was placed in a 25°C heating block, and glycan oxazoline was prepared (100 nmol resuspended in 4.0  $\mu$ L of TGB) and kept on ice. 1  $\mu$ L of the oxazoline solution (25 nmol) was added to the reaction every 10 min for a total of four additions. After a total reaction time of 35 min, the reaction was quenched by dilution with 500  $\mu$ L of cold Protein A binding buffer (100 mM  $\text{Na}_2\text{PO}_4$ , 100 mM NaCl, pH 8.0) and stored at 4°C until confirmation of reaction completion. To the reaction mixture, 100  $\mu$ L rinsed Protein A resin slurry (ThermoFisher Scientific, Cat# 22810) was added and incubated at 4°C, with gentle rocking for 30 min. The solution was then passed through a solid phase extraction tube and washed with cold Protein A binding buffer (0.75 mL); the initial flow through and wash fraction were kept for re-purification by Protein A chromatography if necessary. Resin was then washed with 50 mM sucrose solution in PBS (1.0 mL) to remove unbound glycans, followed by cold Protein A binding buffer (1.0 mL  $\times$  3). Remodelled palivizumab was eluted using 1.0 mL of an elution buffer comprising 20 mM sodium citrate and 100 mM NaCl (pH 3.0) and neutralized with 200  $\mu$ L of Protein A binding buffer. Eluted palivizumab was monitored using SDS-PAGE and purified fractions were combined and buffer exchanged with Histidine/Glycine Buffer (25 mM histidine (Thermo Fisher Scientific Cat#166150250), 1.6 mM glycine (Sigma, Cat# G8898-500 G), pH 6.0). The solutions were stored at 4°C at approximately 0.4–1.0 mg/mL, as quantified by nanodrop (absorbance at 280 nm).

### **Monoclonal antibody characterization**

Reaction progress for glycan remodeling of palivizumab was monitored and characterized using SDS-PAGE. For SDS-PAGE, the samples were reduced in  $\beta$ -mercaptoethanol for 5

min at 100°C, followed by loading onto 10% polyacrylamide gels which were then run at 200 V for 70 min. To ensure accurate analysis of band migration at various glycosylation states, a lane was run comprising both the starting material and the final product within the same lane.

Following palivizumab transglycosylation reactions, remodeled glycans were characterized using PNGase F (New England Biolabs, Cat # P0705S) to release glycans, followed by HPAEC-PAD analysis as detailed below. For analysis using capillary electrophoresis laser-induced fluorescence (CE-LIF), PNGase-released glycans were fluorescently labeled with 8-aminopyrene-1,3,6-trisulfonate (APTS) using the Sciex Fast Glycan Labeling and Analysis Kit (Sciex, Cat.# B94499PTO). Glycans were bound to hydrophilic magnetic beads using a 8:1 ratio of acetonitrile:water. A labeling mixture comprising 7.9  $\mu$ L (40 mM APTS in 20% acetic acid), 1.6  $\mu$ L 0.5% NP-40, 0.8  $\mu$ L (1 M picoline borane in acetonitrile), and 0.8  $\mu$ L maltotriose internal standard was then mixed with the glycan-containing magnetic beads for 1 h at 60°C. Unreacted APTS dye was washed off the beads using 160  $\mu$ L of 8:1 ratio of acetonitrile:water. Analyses were performed as described below. For both CE-LIF and HPAEC-PAD analyses, samples comprising glycans released from intact cetuximab or palivizumab were included in each sequence to also serve as a retention time standard. For CE-LIF, an APTS labeling blank was also included in each sequence to monitor the effects of labeling, and for HPAEC-PAD, a blank comprising diluted buffer was used.

### **Glycan analysis of cetuximab**

For the characterization of cetuximab glycosylation, commercial cetuximab (Erbix®, Imclone LLC/Eli Lilly, DIN#02271249) was purchased from McKesson Pharmacy and buffer exchanged with PBS and concentrated in a 3 kDa MWCO centrifuge tube. To cleave the protein into the Fab and Fc fragments, 1.8 mg/0.4 mL of cetuximab was treated with 1.0  $\mu$ L of IdeZ (New England Biolabs, Cat# P0770S) for 48 h at 37°C. Reaction completion was monitored by SDS-PAGE. The mixture was passed through a Protein A resin column as described above and the unbound fraction containing the  $\text{F(ab')}_2$  fragment was collected. After washing the resin with a binding buffer, the Fc fragment was eluted as described above. The  $\text{F(ab')}_2$  fragment or intact cetuximab were treated with CTAB (TCI America, Cat# H0081)<sup>16</sup> at a final concentration of 5 mg/mL for 5 min at 95°C. After cooling to 37°C, 1.8  $\mu$ L of PNGase F (New England Biolabs, Cat # P0705S) was added to cetuximab or its fragments, and the reaction was left to digest for 24 h. Completion of glycan release was monitored by SDS-PAGE. For purification, samples were cooled on ice to precipitate CTAB. The supernatant was then purified by activated carbon column and eluted with 22% acetonitrile with 0.1% TFA. Following lyophilization and resuspension in MQ water, samples were analyzed by HPAEC-PAD or subsequently labeled for CE-LIF as described above.

### **Glycan analysis by high pH anion-exchange chromatography - pulsed amperometric detection**

HPAEC-PAD analyses were performed on ICS-3000 or ICS-6000 HPAEC PAD instruments (Dionex). For all the methods, Dionex CarboPac PA200 IC columns (3 mm × 250 mm, 5.5 μm particle size, Cat # 062896) and a Gold Standard PAD waveform with an AgCl electrode were used. With exceptions to the analyses of G2(α3)T (**8**) and G2(α6)T (**6**), and PNGase F-cleaved glycans from mAbs, the following method was used for analysis of glycan purity and monitoring of enzymatic reactions: on an ICS-3000 Dionex HPAEC-PAD, a gradient of 20/0/80% to 60/20/20% of MP-A/MP-B/MP-C (MP-A: 200 mM NaOH; MP-B: 150 mM NaOAc in 200 mM NaOH; MP-C: MQ H<sub>2</sub>O) over 10 min at 30°C and 0.4 mL/min was used. For the characterization of G2(α3)T (**8**) and G2(α6)T (**6**) analogues, a modified method was used to improve the peak separation, as follows: a gradient of 20/0/80% to 25/5/70% over 24 min, followed by a gradient to 60/20/20% of MP-A/MP-B/MP-C, respectively, over the next 10 min, at 30°C.

For HPAEC-PAD glycoprofile analyses of PNGase F-cleaved glycans, a flow rate of 0.4 mL/min (at 30°C) and the following gradient was used: 40/0/60% to 35/10/55% of MP-A/MP-B/MP-C over 16.0 or 22.0 min (for ICS-3000 or ICS-6000, respectively), followed by an increase to 35/15/50% over the next 4 min, then 35/20/45% (4 min); for analysis of acidic glycans in cetuximab, a further gradient to 30/30/40% (8 min), followed by 27.2/47/25.8% (8 min) was used. To regenerate the column after each injection, flushes with 0/100/0% (1 min) and then re-equilibration to 40/0/60% over the next 10 min was performed.

### **Glycan analysis and purification by porous graphitic column - high pressure liquid chromatography**

A Dionex U3000 HPLC with HyperCarb columns (Thermo Fisher Cat # 35005-154630, 4.6 mm × 150 mm, 5 μm particle size) or (Thermo Fisher Cat # 35005-159070A, 10 mm × 150 mm, 5 μm particle size) were used for reaction monitoring or purification, respectively, as previously described.<sup>27</sup> Briefly, the following gradient was used for the purification of non-α-galactosylated glycans: the column was first equilibrated to an initial mobile phase composed of 1% MP-D:MP-E (MP-D: 90% acetonitrile in MQ H<sub>2</sub>O containing 0.1% TFA; MP-E:MQ H<sub>2</sub>O containing 0.1% TFA); 1 min after sample injection, a gradient of 6.0% to 13.7% MP-D:MP-E over the next 41.0 min, at 40°C and 5 mL/min. A UV detector (214 nm) was used to monitor glycans, and fractions were collected using a fraction collector. HPAEC-PAD analysis of each fraction was performed to confirm purity and purified fractions were combined and lyophilized. Impure fractions were collected and re-purified.

For α-galactosylated glycans, a modified purification method was used: Following an initial mobile-phase composition of 1% MP-D:MP-E, a gradient of 6.0% to 20.0% MP-D:MP-E was used from 1.0 min to 40.0 min at 40°C. For reaction monitoring, a flow rate of 1.7 mL/min was used, while purification used a flow rate of 5.0 mL/min using their respective columns described above.

### **Glycan analysis by capillary electrophoresis-light induced fluorescence (CE-LIF)**

Samples were analyzed using a Beckman Coulter PA800 plus Pharmaceutical Analysis System equipped with a solid-state laser-induced fluorescence detector ( $\lambda_{ex} = 488 \text{ nm}/\lambda_{em} = 520 \text{ nm}$ ). All separations were carried out using a 60 cm polyvinyl alcohol (PVA) coated capillary (effective length: 50 cm, internal diameter: 50 μm) and a background electrolyte (BGE) buffer consisting of 7.5 mM ammonium acetate pH 4.5, 10% isopropanol. Samples were stored at 10°C and injected hydrodynamically by applying 0.5 psi forward pressure for 10 s (~9 nL). Separations were accomplished at 20°C with an applied voltage of 30 kV in the reversed polarity mode (cathode at injection side). 32Karat (Sciex, version 10.1) was used for data acquisition and processing. To compare glycan profiles, traces were aligned based on the retention time of the APTS-only blank peak.

### **Anti-α1-3-Gal IgE binding assay by ELISA**

Palivizumab analogues comprising α1-3-Gal glycans, and commercially available cetuximab and palivizumab were diluted in 100 mM bicarbonate buffer pH 9.6 and immobilized onto MaxiSorp plates (ThermoFisher, Cat# 439454) overnight at 4°C, at 50 μL/well. Water was added to the outer wells of the plate. Following washing with 0.05% Tween 20 in PBS pH 7.4 (PBS-T) and blocking with 2% bovine serum albumin (bovine serum albumin; Sigma, Cat # A3059-100 G) in PBS-T for 1 h, 100 μL of anti-α1-3-Gal IgE (InBio, 16D9 (Cat#E-16D9, Lot#45328) and 10H8 (Cat# E-10H8, Lot# 45734)) diluted 1/3000 in 2% BSA/PBS-T, was added to each well. Plates were then tightly sealed and incubated for 1.5 h at 37°C. Wells were thoroughly washed with PBS-T, followed by addition of 50 μL of anti-Human IgE Secondary Antibody-HRP (Invitrogen, Cat# PISA510261, Lot #XJ3725591), diluted 1/1000 in 2% BSA/PBS-T. The plates were then gently rocked at room temperature in the dark for 60 min, followed by thorough washing with PBS-T. 50 μL of TMB Substrate (Cell Signal Technologies, Cat# 7004P6) was warmed to room temperature and added, and the plate was gently rocked in the dark for 7-12 min, before quenching with 50 μL of 2 M H<sub>2</sub>SO<sub>4</sub>. Plates were immediately read on a BioTek Plate reader at 450 nm. Normalized absorbance values are reported as values relative to cetuximab control wells at 6.25 μg/mL on each plate. Technical duplicates were performed for each sample on each day, and three experimental replicates were performed for each anti-α-1-3-Gal IgE antibody. Sample locations were randomized where possible for each experimental replicate. The ELISA parameters were optimized using commercial cetuximab to establish linearity (with four points in the linear range,  $R^2 > 0.95$ ); the specificity and reactivity of the 16D9 and 10H8 anti-α1-3-Gal hIgEs toward the α-Gal epitope were validated by the vendor (InBio) using ELISA and immunoblotting. The in-house specificity of the 16D9 and 10H8 IgE antibodies were established using commercial cetuximab as a positive control, and deglycosylated palivizumab, soluble unbound α1-3-Gal glycans, and anti-human IgE-HRP antibodies alone (i.e., without any primary IgE antibodies) as negative controls (Figure S3).

### FcγRIIIA binding assay by ELISA

Recombinant human FcγRIIIA V176 protein (R&D Systems, Cat# 4325-FC-050) was immobilized onto MaxiSorp plates overnight at 4°C, at 50 μL of 2.0 μg/mL. Following washing with PBS-T and blocking with 1% BSA/PBS-T, each palivizumab glycoform was serially diluted fourfold in 1% BSA/PBS-T and 50 μL was added to each well. Plates were gently rocked for 2 h at room temperature. Wells were thoroughly washed with PBS-T, followed by the addition of goat anti-Human IgG F(ab')<sub>2</sub> Secondary Antibody-HRP (50 μL, 1/500 dilution in 1% BSA/PBS-T, ThermoFisher, Cat # PI31482). The plate was then gently rocked at room temperature in the dark for 60 min, followed by thorough washing with PBS-T. Wells were treated with 50 μL TMB substrate incubated for 20 min, stopped with 50 μL 2 M H<sub>2</sub>SO<sub>4</sub> and imaged as above.

### Statistical analysis

All statistical analyses were performed using GraphPad Prism version 9.0.0 (GraphPad Software, San Diego, CA, USA). Non-linear regression (variable slope, four parameters) was used for curve-fitting. All data are presented as mean ± standard deviation.

### Abbreviations

|                   |   |
|-------------------|---|
| α-galactosylation | glycan comprising a terminal α1-3-Gal residue   |
| α1-3-Gal          | terminal galactosyl-α1-3-galactosyl disaccharide moiety   |
| α1-3-GalTase      | α1-3-Galactosyltransferase  |
| ADCC              | antibody-dependent cellular cytotoxicity  |
| APTS              | 8-aminopyrene-1,3,6-trisulfonate  |
| β-galactosylation | glycan comprising a terminal Gal-β1-4-GlcNAc residue  |
| CE-LIF            | capillary electrophoresis – light induced fluorescence  |
| CQAs              | critical quality attributes   |
| CTAB              | cetyltrimethylammonium bromide  |
| Fc                | fragment crystallizable   |
| Fab               | fragment antigen-binding  |
| G1(α3)            | biantennary glycan with α1-3-Gal on the α3 antenna without a terminal Gal-β1-4-GlcNAc on the α6 antenna |
| G1(α6)            | biantennary glycan with α1-3-Gal on the α6 antenna without a terminal Gal-β1-4-GlcNAc on the α3 antenna |
| G2(α3)            | biantennary glycan with α1-3-Gal on the α3 antenna and a terminal Gal-β1-4-GlcNAc on the α6 antenna     |
| G2(α6)            | biantennary glycan with α1-3-Gal on the α6 antenna and a terminal Gal-β1-4-GlcNAc on the α3 antenna     |
| G2(α3,6)          | biantennary glycan with α1-3-Gal on each antenna  |
| Gal               | galactosyl  |

|                  |  |
|------------------|--|
| Gal-β1-4-GlcNAc  | galactosyl-α1-4- <i>N</i> -acetylglucosaminyl disaccharide moiety    |
| GlcNAc           | <i>N</i> -acetylglucosaminyl   |
| HPAEC-PAD        | high pH anion exchange chromatography – pulse amperometric detection |
| IgE              | Immunoglobulin E   |
| IgG              | Immunoglobulin G   |
| MBD-α1-3-GalTase | Maltose-binding domain-conjugated α-1-3-galactosyltransferase        |
| NMR              | nuclear magnetic resonance   |
| Pal-GxF          | palivizumab comprising remodeled Fc glycans of various structures    |
| PBS              | phosphate buffered saline  |
| PGC-HPLC         | porous graphitic column – high performance liquid chromatography     |
| PNaseF           | peptide- <i>N</i> -glycosidase F                                     |
| SDS-PAGE         | sodium dodecyl sulfate – polyacrylamide gel electrophoresis          |
| UDP-Gal          | uridine diphosphate galactose  |

### Acknowledgements

We thank Drs Yves Aubin, Sean Li, Simon Sauvé, and Michael Rosu-Myles for review of this manuscript. We thank Melissa J Schur for help with the preparation of the α1-3 and β1-4 galactosyltransferases.

### Disclosure statement

No potential conflict of interest was reported by the author(s).

### Funding

This work is funded by the Government of Canada.

### ORCID

Roger Y. Tam  <http://orcid.org/0000-0002-8441-6681>

### Author contributions

GH synthesized glycans and remodeled monoclonal antibodies, prepared enzymes, performed HPAEC-PAD and data analysis. LT performed ELISA binding assays. JT and HL performed CE-LIF analyses. MG prepared enzymes and edited the manuscript. RT conceptualized experiments, synthesized glycans, performed HPAEC-PAD and ELISA experiments, data analysis/interpretation, and wrote and edited manuscripts. All authors contributed to the article and approved the submitted version.

### References

- Lu RM, Hwang YC, Liu IJ, Lee CC, Tsai HZ, Li HJ, Wu HC. Development of therapeutic antibodies for the treatment of diseases. *J Biomed Sci.* 2020;27(1):1. doi:10.1186/s12929-019-0592-z. PMID: 31894001.
- Reusch D, Tejada ML. Fc glycans of therapeutic antibodies as critical quality attributes. *Glycobiology.* 2015;25(12):1325–34. doi:10.1093/glycob/cwv065. PMID: 26263923.
- Kunert R, Reinhart D. Advances in recombinant antibody manufacturing. *Appl Microbiol Biotechnol.* 2016;100(8):3451–61. doi:10.1007/s00253-016-7388-9. PMID: 26936774.

4. Durocher Y, Butler M. Expression systems for therapeutic glycoprotein production. *Curr Opin Biotechnol.* 2009;20:700–07. doi:10.1016/j.copbio.2009.10.008. PMID: 19889531.
5. Stadlmann J, Pabst M, Kolarich D, Kunert R, Altmann F. Analysis of immunoglobulin glycosylation by LC-ESI-MS of glycopeptides and oligosaccharides. *Proteomics.* 2008;8(14):2858–71. doi:10.1002/pmic.200700968. PMID: 18655055.
6. Bosques CJ, Collins BE, Meador JW 3rd, Sarvaiya H, Murphy JL, Dellorusso G, Bulik DA, Hsu IH, Washburn N, Sipsey SF, et al. Chinese hamster ovary cells can produce galactose- $\alpha$ -1,3-galactose antigens on proteins. *Nat Biotechnol.* 2010;28(11):1153–56. doi:10.1038/nbt1110-1153. PMID: 21057479.
7. Hinterholzer A, Moises J, Regl C, Schwap S, Rapp E, Huber CG, Schubert M. Unambiguous identification of  $\alpha$ -Gal epitopes in intact monoclonal antibodies by NMR spectroscopy. *MAbs.* 2022;14(1):2132977. doi:10.1080/19420862.2022.2132977. PMID: 36239533.
8. She YM, Dai S, Tam RY. Highly sensitive characterization of non-human glycan structures of monoclonal antibody drugs utilizing tandem mass spectrometry. *Sci Rep.* 2022;12(1):15109. doi:10.1038/s41598-022-19488-8. PMID: 36068283.
9. Maeda E, Kita S, Kinoshita M, Urakami K, Hayakawa T, Kakehi K. Analysis of nonhuman N-glycans as the minor constituents in recombinant monoclonal antibody pharmaceuticals. *Anal Chem.* 2012;84(5):2373–79. doi:10.1021/ac300234a. PMID: 22394092.
10. Galili U. The  $\alpha$ -gal epitope (Gal $\alpha$ 1-3Gal $\beta$ 1-4GlcNAc-R) in xenotransplantation. *Biochimie.* 2001;83(7):557–63. doi:10.1016/s0300-9084(01)01294-9. PMID: 11522383.
11. Jefferis R. Glycosylation as a strategy to improve antibody-based therapeutics. *Nat Rev Drug Discov.* 2009;8(3):226–34. doi:10.1038/nrd2804. PMID: 19247305.
12. Sandrin MS, Vaughan HA, Dabkowski PL, McKenzie IF. Anti-pig IgM antibodies in human serum react predominantly with Gal ( $\alpha$ 1-3)Gal epitopes. *Proc Natl Acad Sci U S A.* 1993;90:11391–95. doi:10.1073/pnas.90.23.11391. PMID: 7504304.
13. Eisenson DL, Hisadome Y, Yamada K. Progress in xenotransplantation: immunologic barriers, advances in gene editing, and successful  $\alpha$ Tolerance induction strategies in pig-to-primate transplantation. *Front Immunol.* 2022;13:899657. doi:10.3389/fimmu.2022.899657. PMID: 35663933.
14. Commins SP, James HR, Kelly LA, Pochan SL, Workman LJ, Perzanowski MS, Kocan KM, Fahy JV, Nganga LW, Ronmark E, et al. The relevance of tick bites to the production of IgE antibodies to the mammalian oligosaccharide galactose- $\alpha$ -1,3-galactose. *J Allergy Clin Immunol.* 2011;127(5):1286–93.e6. doi:10.1016/j.jaci.2011.02.019. PMID: 21453959.
15. Chung CH, Mirakhur B, Chan E, Le QT, Berlin J, Morse M, Murphy BA, Satinover SM, Hosen J, Mauro D, et al. Cetuximab-induced anaphylaxis and ige specific for galactose- $\alpha$ -1,3-galactose. *N Engl J Med.* 2008;358(11):1109–17. doi:10.1056/NEJMoa074943. PMID: 18337601.
16. van Bueren JLL, Rispens T, Verploegen S, van der Palen-Merkus T, Stapel S, Workman LJ, James H, van Berkel PH, van de Winkel JG, Platts-Mills TA, et al. Anti-galactose- $\alpha$ -1,3-galactose IgE from allergic patients does not bind  $\alpha$ -galactosylated glycans on intact therapeutic antibody Fc domains. *Nat Biotechnol.* 2011;29(7):574–76. doi:10.1038/nbt.1912. PMID: 21747378.
17. Qian J, Liu T, Yang L, Daus A, Crowley R, Zhou Q. Structural characterization of N-linked oligosaccharides on monoclonal antibody cetuximab by the combination of orthogonal matrix-assisted laser desorption/ionization hybrid quadrupole-quadrupole time-of-flight tandem mass spectrometry and sequential enzymatic digestion. *Anal Biochem.* 2007;364:8–18. doi:10.1016/j.ab.2007.01.023. PMID: 17362871.
18. Ayoub D, Jabs W, Resemann A, Evers W, Evans C, Main L, Baessmann C, Wagner-Rousset E, Suckau D, Beck A. Correct primary structure assessment and extensive glyco-profiling of cetuximab by a combination of intact, middle-up, middle-down and bottom-up ESI and MALDI mass spectrometry techniques. *MAbs.* 2013;5:699–710. doi:10.4161/mabs.25423. PMID: 23924801.
19. Smith DF, Larsen RD, Mattox S, Lowe JB, Cummings RD. Transfer and expression of a murine UDP-Gal: beta-D-Gal-alpha 1,3-galactosyltransferase gene in transfected Chinese hamster ovary cells. Competition reactions between the alpha 1,3-galactosyltransferase and the endogenous alpha 2,3-sialyltransferase. *J Biol Chem.* 1990;265:6225–34. doi:10.1016/S0021-9258(19)39314-7. PMID: 2108155.
20. Cummings RD, Mattox SA. Retinoic acid-induced differentiation of the mouse teratocarcinoma cell line F9 is accompanied by an increase in the activity of UDP-galactose: beta-D-galactosyl-alpha 1,3-galactosyltransferase. *J Biol Chem.* 1988;263:511–19. doi:10.1016/S0021-9258(19)57422-1. PMID: 3121614.
21. Zhang P, Woen S, Wang T, Liao B, Zhao S, Chen C, Yang Y, Song Z, Wormald MR, Yu C, et al. Challenges of glycosylation analysis and control: an integrated approach to producing optimal and consistent therapeutic drugs. *Drug Discov Today.* 2016;21:740–65. doi:10.1016/j.drudis.2016.01.006. PMID: 26821133.
22. Garcia JJ, Raez LE, Rosas D. A narrative review of biosimilars: a continued journey from the scientific evidence to practice implementation. *Transl Lung Cancer Res.* 2020;9:2113–19. doi:10.21037/tlcr-20-601. PMID: 33209630.
23. Goel N, Chance K. Biosimilars in rheumatology: understanding the rigor of their development. *Rheumatol (Oxford).* 2017;56:187–97. doi:10.1093/rheumatology/kew206. PMID: 27241704.
24. Schiestl M, Stangler T, Torella C, Cepeljnik T, Toll H, Grau R. Acceptable changes in quality attributes of glycosylated biopharmaceuticals. *Nat Biotechnol.* 2011;29:310–12. doi:10.1038/nbt.1839. PMID: 21478841.
25. Wang LX, Tong X, Li C, Giddens JP, Li T. Glycoengineering of antibodies for modulating functions. *Annu Rev Biochem.* 2019;88:433–59. doi:10.1146/annurev-biochem-062917-012911. PMID: 30917003.
26. Parsons TB, Struwe WB, Gault J, Yamamoto K, Taylor TA, Raj R, Wals K, Mohammed S, Robinson CV, Benesch JL, et al. Optimal synthetic glycosylation of a therapeutic antibody. *Angew Chem Weinheim Bergstr Ger.* 2016;128:2407–13. doi:10.1002/ange.201508723. PMID: 27546920.
27. Hatfield G, Tepliakova L, Gingras G, Stalker A, Li X, Aubin Y, Tam RY. Specific location of galactosylation in an afucosylated antiviral monoclonal antibody affects its Fc $\gamma$ RIIIA binding affinity. *Front Immunol.* 2022;13:972168. doi:10.3389/fimmu.2022.972168. PMID: 36304448.
28. Aoyama M, Hashii N, Tsukimura W, Osumi K, Harazono A, Tada M, Kiyoshi M, Matsuda A, Ishii-Watabe A. Effects of terminal galactose residues in mannose  $\alpha$ 1-6 arm of Fc-glycan on the effector functions of therapeutic monoclonal antibodies. *MAbs.* 2019;11(5):826–36. doi:10.1080/19420862.2019.1608143. PMID: 30990348.
29. Fan JQ, Kondo A, Kato I, Lee YC. High-performance liquid chromatography of glycopeptides and oligosaccharides on graphitized carbon columns. *Anal Biochem.* 1994;219:224–29. doi:10.1006/abio.1994.1261. PMID: 8080079.
30. She YM, Tam RY, Li X, Rosu-Myles M, Sauve S. Resolving isomeric structures of native glycans by nanoflow porous graphitized carbon chromatography–mass spectrometry. *Anal Chem.* 2020;92(20):14038–46. doi:10.1021/acs.analchem.0c02951. PMID: 32960038.
31. Elices MJ, Goldstein IJ. Biosynthesis of Bi-, Tri-, and tetraantennary oligosaccharides containing  $\alpha$ -D-Galactosyl residues at their nonreducing termini. *J Biol Chem.* 1989;264(3):1375–80. doi:10.1016/S0021-9258(18)94197-9. PMID: 2492275.
32. Johnson LS, Braden B, inventors; MedImmune Inc., Bowie State University, assignees. Crystals and Structure of Synagis FAB. United States patent US 6,955,717 B2 2005 Oct 18.
33. Li T, Tong X, Yang Q, Giddens JP, Wang LX. Glycosynthase mutants of endoglycosidase S2 show potent transglycosylation activity and remarkably relaxed substrate specificity for antibody glycosylation remodeling. *J Biol Chem.* 2016;291:16508–18. doi:10.1074/jbc.M116.738765. PMID: 27288408.

34. Mariotte D, Dupont B, Gervais R, Galais MP, Laroche D, Tranchant A, Comby E, Bouhier-Leporrier K, Reimund JM, Le Mauff B. Anti-cetuximab IgE ELISA for identification of patients at a high risk of cetuximab-induced anaphylaxis. *MAbs*. 2011;3:396–401. doi:10.4161/mabs.3.4.16293. PMID: 21654207.
35. Dupont B, Mariotte D, Dugue AE, Clarisse B, Grellard JM, Babin E, Chauffert B, Dakpe S, Moldovan C, Bouhier-Leporrier K, et al. Utility of serum anti-cetuximab immunoglobulin E levels to identify patients at a high risk of severe hypersensitivity reaction to cetuximab. *Br J Clin Pharmacol*. 2017;83:623–31. doi:10.1111/bcp.13140. PMID: 27662818.
36. Serrier J, Davy JB, Dupont B, Clarisse B, Parienti JJ, Petit G, Khoy K, Ollivier Y, Gervais R, Mariotte D, et al. Validation of an anti- $\alpha$ -Gal IgE fluoroenzyme-immunoassay for the screening of patients at risk of severe anaphylaxis to cetuximab. *Bmc Cancer*. 2023;23(1):32. doi:10.1186/s12885-023-10501-5. PMID: 36624467.
37. Fussl F, Trappe A, Carillo S, Jakes C, Bones J. Comparative elucidation of cetuximab heterogeneity on the intact protein level by cation exchange chromatography and capillary electrophoresis coupled to mass spectrometry. *Anal Chem*. 2020;92:5431–38. doi:10.1021/acs.analchem.0c00185. PMID: 32105056.
38. Lippold S, Nicolardi S, Wuhler M, Falck D. Proteoform-resolved fc $\gamma$ RIIIa binding assay for fab glycosylated monoclonal antibodies achieved by affinity chromatography mass spectrometry of Fc moieties. *Front Chem*. 2019;7:698. doi:10.3389/fchem.2019.00698. PMID: 31709228.
39. Ruhaak LR, Zauner G, Huhn C, Bruggink C, Deelder AM, Wuhler M. Glycan labeling strategies and their use in identification and quantification. *Anal Bioanal Chem*. 2010;397:3457–81. doi:10.1007/s00216-010-3532-z. PMID: 20225063.
40. Smith SA, Chruszcz M, Chapman MD, Pomes A. Human monoclonal ige antibodies—a major milestone in allergy. *Curr Allergy Asthma Rep*. 2023;23(1):53–65. doi:10.1007/s11882-022-01055-w. PMID: 36459330.
41. Wurth MA, Hadadianpour A, Horvath DJ, Daniel J, Bogdan O, Goleniewska K, Pomes A, Hamilton RG, Peebles RS Jr., Smith SA. Human IgE mAbs define variability in commercial Aspergillus extract allergen composition. *JCI Insight*. 2018;3. doi:10.1172/jci.insight.123387. PMID: 30333320.
42. Khatri K, Richardson CM, Glesner J, Kapingidza AB, Mueller GA, Zhang J, Dolamore C, Vailes LD, Wunschmann S, Peebles RS Jr., et al. Human IgE monoclonal antibody recognition of mite allergen Der p 2 defines structural basis of an epitope for IgE cross-linking and anaphylaxis in vivo. *PNAS Nexus*. 2022;1(3):c054. doi:10.1093/pnasnexus/pgac054. PMID: 35799831.
43. Hadadianpour A, Daniel J, Zhang J, Spiller BW, Makaraviciute A, DeWitt AM, Walden HS, Hamilton RG, Peebles RS Jr., Nutman TB, et al. Human IgE mAbs identify major antigens of parasitic worm infection. *J Allergy Clin Immunol*. 2022;150(6):1525–33. doi:10.1016/j.jaci.2022.05.022. PMID: 35760390.
44. Savitz J, Geaney C, Banks TA. A case of anaphylaxis to palivizumab. *Ann Allergy Asthma Immunol*. 2014;113:236–37. doi:10.1016/j.anaai.2014.06.006. PMID: 25065351.
45. Resch B. Product review on the monoclonal antibody palivizumab for prevention of respiratory syncytial virus infection. *Hum Vaccin Immunother*. 2017;13:2138–49. doi:10.1080/21645515.2017.1337614. PMID: 28605249.
46. Deisenhofer J. Crystallographic refinement and atomic models of a human Fc fragment and its complex with fragment B of protein a from *Staphylococcus aureus* at 2.9- and 2.8-Å resolution. *Biochemistry*. 1981;20(9):2361–70. doi:10.1021/bi00512a001. PMID: 7236608.
47. Barb AW, Prestegard JH. NMR analysis demonstrates immunoglobulin G N-glycans are accessible and dynamic. *Nat Chem Biol*. 2011;7:147–53. doi:10.1038/nchembio.511. PMID: 21258329.
48. Yamaguchi Y, Kato K, Shindo M, Aoki S, Furusho K, Koga K, Takahashi N, Arata Y, Shimada I. Dynamics of the carbohydrate chains attached to the Fc portion of immunoglobulin G as studied by NMR spectroscopy assisted by selective <sup>13</sup>C labeling of the glycans. *J Biomol NMR*. 1998;12:385–94. doi:10.1023/a:1008392229694. PMID: 9835046.
49. Barb AW, Brady EK, Prestegard JH. Branch-specific sialylation of IgG-Fc glycans by ST6Gal-I. *Biochemistry*. 2009;48:9705–07. doi:10.1021/bi901430h. PMID: 19772356.
50. Lungulescu CV, Ungureanu BS, Turcu-Stolica A, Ghimpau V, Artene SA, Cazacu IM, Grecu AF, Dinescu VC, Croitoru A, Volovat SR. The role of IgE specific for galactose- $\alpha$ -1,3-galactose in predicting cetuximab induced hypersensitivity reaction: a systematic review and a diagnostic meta-analysis. *Sci Rep*. 2020;10(1):21355. doi:10.1038/s41598-020-78497-7. PMID: 33288791.
51. Subedi GP, Hanson QM, Barb AW. Restricted motion of the conserved immunoglobulin G1 N-Glycan is essential for efficient Fc $\gamma$ RIIIa binding. *Structure*. 2014;22(10):1478–88. doi:10.1016/j.str.2014.08.002. PMID: 25199692.
52. Crispin M, Yu X, Bowden TA. Crystal structure of sialylated IgG Fc: implications for the mechanism of intravenous immunoglobulin therapy. *Proc Natl Acad Sci U S A*. 2013;110:E3544–3546. doi:10.1073/pnas.1310657110. PMID: 23929778.
53. Van Coillie J, Schulz MA, Bentlage AEH, de Haan N, Ye Z, Geerdes DM, van Esch WJE, Hafkenschied L, Miller RL, Narimatsu Y, et al. Role of N-Glycosylation in Fc $\gamma$ RIIIa interaction with IgG. *Front Immunol*. 2022;13:987151. doi:10.3389/fimmu.2022.987151. PMID: 36189205.
54. Li T, DiLillo DJ, Bournazos S, Giddens JP, Ravetch JV, Wang LX. Modulating IgG effector function by Fc glycan engineering. *Proc Natl Acad Sci USA*. 2017;114:3485–90. doi:10.1073/pnas.1702173114. PMID: 28289219.
55. Sjogren J, Struwe WB, Cosgrave EF, Rudd PM, Stervander M, Allhorn M, Hollands A, Nizet V, Collin M. EndoS2 is a unique and conserved enzyme of serotype M49 group *Streptococcus* that hydrolyses N-linked glycans on IgG and  $\alpha$ 1-acid glycoprotein. *Biochem J*. 2013;455(1):107–18. doi:10.1042/BJ20130126. PMID: 23865566.